.....contributing to man's
understanding of the environment world

JOINT MAGNITUDE DETERMINATION AND ANALYSIS OF VARIANCE FOR EXPLOSION MAGNITUDE ESTIMATES

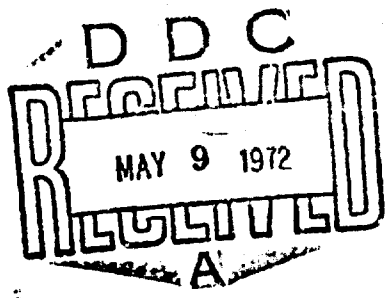

D. H. VON SEGGERN
SEISMIC DATA LABORATORY

13 JANUARY 1972

Prepared for
AIR FORCE TECHNICAL APPLICATIONS CENTER
Washington, D.C.

Under
Project VELA UNIFORM

Sponsored by
ADVANCED RESEARCH PROJECTS AGENCY
Nuclear Monitoring Research Office
ARPA Order No. 1714

TELEDYNE GEOTECH
ALEXANDRIA LABORATORIES

Neither the Advanced Research Projects Agency nor the Air Force Technical Applications Center will be responsible for information contained herein which has been supplied by other organizations or contractors, and this document is subject to later revision as may be necessary. The views and conclusions presented are those of the authors and should not be interpreted as necessarily representing the official policies, either expressed or implied, of the Advanced Research Projects Agency, the Air Force Technical Applications Center, or the U S Government.

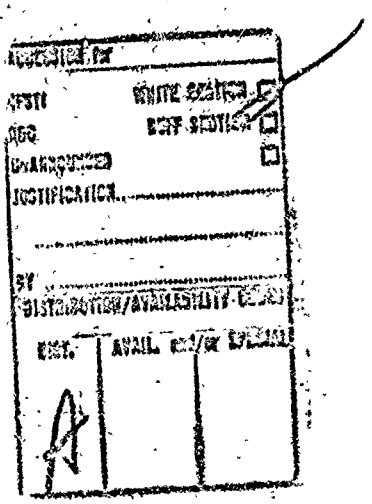

JOINT MAGNITUDE DETERMINATION AND ANALYSIS OF VARIANCE FOR EXPLOSION MAGNITUDE ESTIMATES

SEISMIC DATA LABORATORY REPORT NO. 286

AFTAC Project No.:	VELA T/2706
Project Title:	Seismic Data Laboratory
ARPA Order No.:	1714
ARPA Program Code No.:	2F-10
Name of Contractor:	TELEDYNE GEOTECH
Contract No.:	F33657-72-C-0009
Date of Contract:	01 July 1971
Amount of Contract:	$ 1,314,000
Contract Expiration Date:	30 June 1972
Project Manager:	Royal A. Hartenberger (703) 836-7647

P. O. Box 334, Alexandria, Virginia

ABSTRACT

A method of relative magnitude determination using all available data for a limited source area is proposed. The attenuation factor B, event terms F_j, and station terms C_i for the linear model

$$X_{ij} = C_i + F_j + H - BR_{ij}$$

are solved simultaneously by an iterative least-squares procedure; here X_{ij} is the logarithm of the amplitude and R_{ij} is the logarithm of the distance. The method is analogous to joint epicenter determination, and so is termed "joint magnitude determination" (JMD). Since observed amplitudes, either body wave or surface wave, seldom are seen to follow a straight-line decay, the model is a gross simplification in which the station terms actually operate somewhat as distance-correction terms. The JMD method was applied to Seismic Data Laboratory (SDL) data from North American stations for Nevada Test Site explosions. The standard deviation of station magnitudes (M_s and m_b) computed by JMD for an event typically was one-half of the standard deviation of magnitudes computed by routine methods. This reduction is wholly due to the addition of station terms. Surprisingly, no consequent reduction in scatter of the explosion M_s vs m_b plot was attained by using JMD estimates rather than routine ones, and it is concluded that source parameters rather than bias due to varying networks is causing the scatter. The scatter of magnitude estimates is divided into three physically meaningful

parts: source, path-station, and measurement. The absolute value for each part is derived from the seismic measurements without using yield information.

TABLE OF CONTENTS

LIST OF FIGURES

LIST OF FIGURES (Cont'd.)

LIST OF TABLES

INTRODUCTION

Estimation of event magnitude, either M_s or m_b, has always been hampered by the inability to provide a uniform distance-correction function which will apply satisfactorily to all source areas. Especially at regional distances, application of generalized distance corrections can introduce extreme bias into magnitude estimates. Therefore, seismologists have devised a number of disparate magnitude formulas and distance-correction functions or tables (Båth, 1966 and 1969; VESIAC, 1964). For example, in the Western United States detailed analysis of the earth structure and travel times enabled Evernden (1967) to formulate appropriate m_b formulas; and a study of Rayleigh wave amplitudes from NTS events by von Seggern (1970) led to a regional M_s distance-correction function for the Western United States. In these and similar studies, the object was to devise a set of formulas which would cover a considerable distance range so that recorded amplitudes at given distances could be equalized by use of the appropriate formula.

There are three disadvantages to the above approach: 1) the determined formulas are tied to a certain area and cannot be reliably applied elsewhere when either epicenters or travel paths are changed; 2) the amplitude analysis required to establish the formulas can be lengthy and complicated; and 3) the formulas can be awkward to apply in practice when the distance range has been segmented. Tabulated distance-correction terms for

magnitude have nearly the same deficiencies.

Thus, we believe a simpler approach is demanded. What we propose is to establish, using the NTS data, single amplitude-distance functions for M_s and for m_b. Rather than attempting to fit the observed amplitudes as closely as possible with a segmented formula, we will invoke station terms to reduce the deviations from the single amplitude-distance functions. These station terms should not be considered to be intimately connected with the immediate structure at the station, but to be the cumulative effect of the entire travel path on the recorded amplitude at a given site. Since we employ station terms, it may then be argued that this approach also is limited to a small source area and certain propagation paths. However, this simple approach can be applied to area after area with ease, new station corrections and a new amplitude-distance function being generated each time from the available data. Since it has been established that the M_s vs m_b discriminant should be regionalized (Liebermann and Pomeroy, 1969), this magnitude determination approach is especially convenient in monitoring particular source areas where relative values of M_s or m_b between areas need not be established. We are interested in determining whether this approach can produce M_s vs m_b data which is as good as or better than data provided by use of more conventional magnitude calculations. The addition of station terms should reduce the variance of individual magnitude values for an event and should improve the scatter in M_s vs m_b plots. In this report, we reprocess

the data used by Lambert (1971) in establishing the M_s vs m_b relation for the Nevada Test Site in order to compare this new approach to routine magnitude estimation.

METHOD OF JOINT MAGNITUDE DETERMINATION

This method is intended to compare magnitudes of individual events in a particular source area recorded by several stations. The station set need not be the same for each event, but some stations should be common to several of the events.

The following description of the method of obtaining the magnitude formula pertains to both M_s and m_b. As the amplitude-distance model for both, we use an exponential decay function which approximates the real data reasonably, as will be seen later:

$$x_{ij} = c_i \, f_j \, h \, r_{ij}^{-B}$$

where

x_{ij} = the calculated amplitude at station i for event j,
c_i = the station factor,
f_j = the event factor,
h = a constant for a particular data set,
r_{ij} = the distance to station i from event j,
B = a constant for a particular data set.

Linearize the equation by taking the logarithm of both sides:

$$\log x_{ij} = \log c_i + \log f_j + \log h - B \log r_{ij}$$

Rewrite the equation in this simple manner:

$$\hat{X}_{ij} = \hat{C}_i + \hat{F}_j + \hat{H} + \hat{B}R_{ij}$$

where the substitutions are evident. Here and henceforth, the carat symbol denotes an estimate. Now let Z_{ij} be the log of the observed amplitude; then form the error equation:

$$\hat{E}_{ij} = Z_{ij} - \hat{C}_i - \hat{F}_j - \hat{H} + \hat{B}R_{ij} \qquad (1)$$

One could, at this point, construct the normal equations for this overdetermined linear system and solve explicitly for the $\hat{B}$, $\hat{H}$, $\hat{C}_i$'s and $\hat{F}_j$'s which minimize the sum of the squares of (1). However, it was judged that the matrices to be inverted would be too large (nearly 200 x 200 for the data used in this report) to handle accurately or efficiently; and we used the following iterative scheme, based on analytic solutions of the least-squares problem. This scheme allows us to solve for up to a combined total of 200 station and event terms, plus $\hat{B}$ and $\hat{H}$, in less than two minutes of computer time. We desire to minimize:

$$\sum_{ji}\hat{E}_{ij}^2 = \sum_{ji}W_{ij}(Z_{ij} - \hat{C}_i - \hat{F}_j - \hat{H} + \hat{B}R_{ij})^2 \qquad (2)$$

where W_{ij} is a weighting factor, equal to one if station i recorded event j or to zero if it did not. By expanding the right-hand side of (2), taking derivatives with respect to $\hat{B}$, and setting the result equal to zero, we obtain:

$$\hat{B} = \frac{\hat{H}\sum_{ji}W_{ij}R_{ij} + \sum_j\hat{F}_j\sum_i W_{ij}R_{ij} + \sum_i\hat{C}_i\sum_j W_{ij}R_{ij} - \sum_{ji}W_{ij}Z_{ij}R_{ij}}{\sum_{ji}W_{ij}R_{ij}^2} \qquad (3)$$

Similarly, we obtain for H:

$$\hat{H} = \frac{\hat{B}\sum_{ji}\sum W_{ij}R_{ij} + \sum_{ji}\sum W_{ij}Z_{ij} - \sum_{ji}\sum W_{ij}\hat{F}_j - \sum_{ji}\sum W_{ij}\hat{C}_i}{\sum_{ji}\sum W_{ij}} \tag{4}$$

By substituting equation (4) in (3), we obtain an expression for B which depends on only the given data plus station and event terms:

$$\hat{B} = \frac{[(\sum_{ji}\sum W_{ij}R_{ij})(\sum_{ji}\sum W_{ij}Z_{ij} - \sum_{ji}\sum W_{ij}\hat{F}_j - \sum_{ji}\sum W_{ij}\hat{C}_i)}{(\sum_{ji}\sum W_{ij})(\sum_{ji}\sum W_{ij}R_{ij}^2) - (\sum_{ji}\sum W_{ij}R_{ij})^2} \tag{5}$$

$$\frac{- (\sum_{ji}\sum W_{ij})(\sum_{ji}\sum W_{ij}Z_{ij}R_{ij} - \sum_{ji}\sum \hat{F}_j \sum_i W_{ij}R_{ij} - \sum_{ji}\sum \hat{C}_i \sum_j W_{ij}R_{ij})]}{}$$

To derive least-squares expressions for the $\hat{F}_j$'s and $\hat{C}_i$'s we must sum equation (2) over j or i only, respectively. Expanding (2) with the j summation, taking the derivatives with respect to $\hat{F}_j$, and equating to zero gives:

$$\hat{F}_j = \frac{\hat{B}\sum_i W_{ij}R_{ij} + \sum_i W_{ij}Z_{ij} - \hat{H}\sum_i W_{ij} - \sum_i W_{ij}\hat{C}_i}{\sum_i W_{ij}} \tag{6}$$

Similarly, we obtain for $\hat{C}_i$:

$$\hat{C}_i = \frac{\hat{B}\sum_j W_{ij}R_{ij} + \sum_j W_{ij}Z_{ij} - \hat{H}\sum_j W_{ij} - \sum_j W_{ij}\hat{F}_j}{\sum_j W_{ij}} \tag{7}$$

The $\hat{B}$, $\hat{H}$, $\hat{F}_j$'s and $\hat{C}_i$'s are not independent and must be arrived at iteratively. One would like to start with some initial approximate values for the $\hat{F}_j$'s and

$\hat{C}_i$'s. However, in most cases the $\hat{C}_i$'s will be unknown or only crudely known, and in practice one can safely start by setting all $\hat{C}_i$'s equal to zero. Initial $\hat{F}_j$'s may be available from routine magnitude calculations at one or more stations for all the events. In practice, it was found that the program converged to equivalent solutions regardless of the accuracy of these initial $\hat{F}_j$'s; they in fact can also be safely set to zero at the start of the iterative solution. We found that the final values of the $\hat{F}_j$'s and of $\hat{H}$ reflected the initial values; that is, if all $\hat{F}_j$'s are initially overestimated, the final $\hat{F}_j$'s will be overestimated with a consequent adjustment in $\hat{H}$.

Equations (5) and (6) show that the intercept $\hat{H}$ and the slope $\hat{B}$ are dependent on the distance-sensitive $\hat{C}_i$ terms. It was found that estimation of $\hat{H}$ and $\hat{B}$ must be isolated from calculation of the $\hat{C}_i$'s to obtain convergence of the solutions. This is done by using:

$$\hat{B} = \frac{\left[\left(\sum_{ji}\sum W_{ij}R_{ij}\right)\left(\sum_{ji}\sum W_{ij}Z_{ij} - \sum_{ji}\sum W_{ij}\hat{F}_j\right) - \left(\sum_{ji}\sum W_{ij}\right)\left(\sum_{ji}\sum W_{ij}R_{ij}^2\right) - \left(\sum_{ji}\sum W_{ij}R_{ij}\right)^2\right.}{\left.\left(\sum_{ji}\sum W_{ij}\right)\left(\sum_{ji}\sum W_{ij}Z_{ij}R_{ij} - \sum_j \hat{F}_j \sum_i W_{ij}R_{ij}\right)\right]} \tag{8}$$

$$\hat{H} = \frac{\hat{B}\sum_{ji}\sum W_{ij}R_{ij} + \sum_{ji}\sum W_{ij}Z_{ij} - \sum_{ji}\sum W_{ij}\hat{F}_j}{\sum_{ji}\sum W_{ij}} \tag{9}$$

The program iterates through equations (8), (9), (6), and (7), in that order, until changes in the solutions are negligible. A final iteration then returns to equations (5) and (4) to estimate $\hat{B}$ and $\hat{H}$; the value of the additional terms in (8) and (9) as compared to (5) and (4) are then relatively small and do not really change $\hat{B}$ or $\hat{H}$ significantly.

We now point out the analogy between this method for obtaining station magnitude terms together with source magnitudes and the Joint Epicenter Determination method of Douglas (1967) for simultaneously determining station corrections to travel time and epicenter corrections to preliminary estimates. Because of the similarity, we refer to our method as Joint Magnitude Determination (JMD).

APPLICATION TO NTS COMPRESSIONAL-WAVE AND RAYLEIGH-WAVE DATA

The staff of SDL has analyzed and tabulated seismic data on 79 NTS underground shots (FAULTLESS excluded) recorded at over 300 stations. We will employ the JMD program on the compressional-wave (P_n and P) and Rayleigh-wave amplitudes and solve for $\hat{B}$, $\hat{H}$, $\hat{F}_j$'s and $\hat{C}_i$'s in both cases. Note that by "amplitude" we mean the particle displacement (A) and not the particle velocity (A/T) which is often referred to as "amplitude" and routinely used in magnitude calculations at the SDL and elsewhere. It was shown by von Seggern (1970) that the displacement measure had a smaller variance than the velocity measure at least for Rayleigh waves. We will show this again with results of JMD; and also in this section we will investigate the possibility of using the maximum trace amplitude divided by the system magnification at the calibration period ($\overline{A}$), regardless of observed period, another measure considered by von Seggern (1970).

Rayleigh-wave data

Only 45 of the 79 shots had reported Rayleigh-wave amplitudes. There were 712 measurements available to begin with. Through previous experience with the data, we felt that many of the measurements, while not anomalous in a real sense, are in fact erroneous due to calibration errors, analysts' error, transcription or keypunch errors, etc. It was therefore desirable to

eliminate the tails of the data distribution. First, M_s was computed in the routine manner using our formula (von Seggern, 1970) for $\Delta<15°$ and Gutenberg's formula for $\Delta>15°$. The average magnitude for each event was determined, and then all measurements which produced a station magnitude more than one unit from the average were deleted. Fifteen measurements were discarded in this way. Three additional measurements were discarded because they essentially duplicated another site for an event (e.g., ST1TX discarded while ST2TX retained). A different situation occurred with LRSM stations which were repositioned during their recording career; such stations are considered to be the same (e.g., HL-ID and HL2ID); and all the measurements were retained under one station name. Two more measurements were discarded when two events (both having just one reported amplitude) were re-examined: (1) DES MOINES - an excursion at KN-UT which was apparently picked originally as a Rayleigh wave is spurious because its period and travel time do not coincide with other shots and (2) MINK - a Rayleigh wave picked at HL-ID must really be from the Vancouver earthquake of about the same origin time. After all these deletions, 692 measurements remained for 43 events. Program JMD was then run on this data. Initial input estimates of the $\hat{F}_j$'s were taken from SDL's previous magnitude estimates, except a constant was subtracted so that they would be distributed with approximately zero mean; and the initial estimates of the $\hat{C}_i$'s were all zero. It was felt that some additional truncation of the tails of the data based on their statistical distribution as determined by the JMD program was desirable. The

deviations of individual magnitude estimates using

$$\hat{F}_{ij} = Z_{ij} - \hat{H} - \hat{C}_i + \hat{B}R_{ij} \qquad (10)$$

from the $\hat{F}_j$ term for the j'th event appeared to be normally distributed; on this assumption the standard deviation was calculated to be 0.16. All measurements which resulted in a value of $(\hat{F}_{ij} - \hat{F}_j)$ greater than approximately twice the standard deviation of the $\hat{F}_{ij}$'s ($\pm$ 0.35 was actually chosen) were discarded; these totaled 19 measurements. At this point six stations outside North America, each recording Rayleigh waves from only one event, were discarded from the data base. These were OO-NW, TE-GL, FH-PN, AD-IS, HW-IS, and GG-GR. It is important to mention that the two island stations AD-IS and HW-IS had magnitudes $\hat{F}_{ij}$ (before station corrections were applied) of approximately 0.6 and 0.8 below their respective event terms $\hat{F}_j$; this anomalous character may be due to the primarily oceanic paths from NTS. After these deletions, 667 measurements were left for 43 events. Program JMD was run again, and this time three measurements fell over the $\pm$ 0.35 criterion, due to slight readjustments in station and event terms. These three were discarded, and the final run of JMD produced no measurements over the $\pm$ 0.35 criterion. In all, we have thus discarded approximately 5 per cent of the data because they were anomalous and possibly erroneous. The final values of $\hat{B}$ and $\hat{H}$ were 0.90 and 4.55 respectively, with a 95 per cent confidence interval of $\pm$ 0.03 on the slope $\hat{B}$. The final event

terms (equivalent to M_s) are given in Table I, and the final station terms are given in Table II. Thus, for Rayleigh waves from NTS to North American stations, we have this unified distance relation by substitution of the calculated slope and intercept into the original model:

$$\log A_{ij} = 4.55 - 0.90 \log r_{ij} + \hat{F}_j + \hat{C}_i$$

where A is amplitude in millimicrons (peak-to-peak) and r is epicentral distance in degrees. In Figure 1a we show a plot of the logarithm of observed amplitudes normalized by the event term, $\log(A_{ij}) - \hat{F}_j$, versus $\log r_{ij}$ (not all 664 points are shown since some symbols represent more than one data point in this computer printout plot routine). In Figure 1b we show the same data corrected by the station term, $\log(A_{ij}) - \hat{F}_j - \hat{C}_i$, versus $\log r_{ij}$. It is evident that the addition of the station terms greatly decreases the scatter of the data.

The 0.90 exponential decay of the Rayleigh-wave amplitude data deserves discussion. Gutenberg (1945) suggested 1.66 for teleseismic data ($\Delta > 15°$), but Figures 1a and 1b do not show a tendency for the North American data to approach this value, even for the teleseismic range from NTS. Our present result is less than the revised slope of 1.09 for regional distances using the same NTS Rayleigh-wave data (von Seggern, 1970); however, that value was arrived at by an entirely different means. Our result does agree very well with that of Basham (1971), however. Such a slow decay as $r^{-.90}$ can only be explained by a relatively high Q along the travel path of Rayleigh waves at periods of about 12-18

TABLE I

Rayleigh-wave Event Terms

EVENT	F	NUMBER OF STATIONS
AUK	- .45	21
BENHAM	1.60	7
BILBY	.84	28
BOURBON	.17	11
BOXCAR	1.71	14
BRONZE	.15	27
BUFF	- .08	20
CHARCOAL	- .34	17
CHARTREUSE	.04	18
COMMODORE	.86	16
CORDUROY	.48	21
CUP	- .07	24
DILUTED WATERS	- .96	14
DUMONT	.41	18
DURYEA	- .10	16
*FISHER	-1.26	1
FORE	- .22	28
GREELEY	1.49	19
HARDHAT	- .63	31
HAYMAKER	- .41	16
HALFBEAK	1.11	14
KLICKITAT	- .24	25
KNICKERBOCKER	.51	11
*MADISON	- .68	3
MARSHMALLOW	-1.09	5
MERRIMEC	- .96	7
MISSISSIPPI	- .32	34
NASH	- .13	6
*PAMPAS	- .60	2
PALANQUIN	-1.21	10
*PAR	-1.25	16
PILEDRIVER	.23	18
PINSTRIPE	- .82	11
*REDHOT	-1.41	1
REX	- .12	9
SCOTCH	.83	16
SCROLL	-1.23	5
*SEDAN	- .32	20
*STUTZ	-1.40	3
TAN	.24	20
TURF	- .28	31
WAGTAIL	- .10	19
WISHBONE	-1.04	11

*Not used in M_s vs m_b fit.

TABLE II

Rayleigh-Wave Station Terms

STATION	C	NUMBER OF EVENTS
AE-NC	.08	1
AN-MA	-.06	1
AR-WS	-.02	2
AT-NV	-.29	2
AX2AL	-.11	8
AY-SD	-.34	1
AZ-TX	-.20	3
BE-FL	.02	9
BF-CL	.12	2
BG-ME	.17	1
BL-WV	-.04	6
BMO	-.11	20
BM-TX	.39	1
BR-PA	.42	6
BX-UT	.12	3
CG-VA	.20	1
CPO	.17	15
CP-CL	.10	8
CR-NB	.28	10
CU-NV	.03	1
CV-TN	-.01	1
DH-NY	.24	8
DR-CO	-.15	9
DU-OK	-.28	3
DV-CL	-.41	2
EB-MT	-.16	2
EF-TX	.07	1
EK-NV	-.32	4
EN-MO	.12	3
EP-TX	.15	1
EU2AL	.07	4
EY-NV	.27	1
FK-CO	.33	6
FM-UT	-.25	3
FR-MA	-.09	4
FS-AZ	.02	6
GD-VA	-.12	1
GE-AZ	.10	8
GI-MA	-.17	3
GN-NM	.21	1
GR2TX	.34	2
GV-TX	.19	13
HB-OK	.09	4
HH-ND	-.09	3
HK-WY	-.24	1
HL2ID	-.07	15
HN-ME	-.20	20
HR-AZ	.15	8
HT-NM	-.14	1
HV-MA	-.18	2
HY-MA	-.03	2
JE-LA	.44	3
JP-AT	-.02	8
JR-AZ	.01	10
KC-MO	.20	11
KG-AZ	-.14	1
KM-CL	.02	2
KN-UT	-.02	38
LAO	-.30	2
LC-NM	.21	17
LG-AZ	.09	10
LP-TX	.08	1
LS-NH	.39	3
LV-LA	.22	2
MM-TN	.19	3
MN-NV	.10	34
MO-ID	-.17	6
MP-AR	.09	3
MU-WA	.33	1
MV-CL	.09	8
ND-CL	.20	2
NL2AZ	.20	9
NP-NT	.01	18
PG-BC	-.10	11
PI-WY	-.19	1
PM-WY	-.08	3
PT-OR	-.05	3
RG-SD	-.09	9
RK-ON	-.20	18
RT-NM	-.15	8
RY-ND	-.56	2
SA4TX	.33	2
SE-MN	.03	2
SF-AZ	.37	1
SG-AZ	.02	9
SI-BC	.14	5
SJ-TX	.08	3
SK-TX	-.23	3
SN-AZ	.14	8
SS-TX	.04	4
ST1TX	.34	2
SV-AZ	-.45	1
SV3QB	-.24	15
SW-MA	-.10	9
TC-NM	.10	1
TFO	.01	24
TF-CL	-.11	4
TK-WA	-.20	3
TN-CL	-.14	1
TU-PA	.42	1
UBO	-.25	20
VN-UT	-.62	1
VO-IO	.18	1
VT-OR	-.43	1
WF-MN	.23	1
WH2YK	.12	7
WI-NV	.04	8
WMO	-.21	17
WM-AZ	.06	1
WN-SD	-.10	10
WO-AZ	.12	8
WW-UT	-.29	1

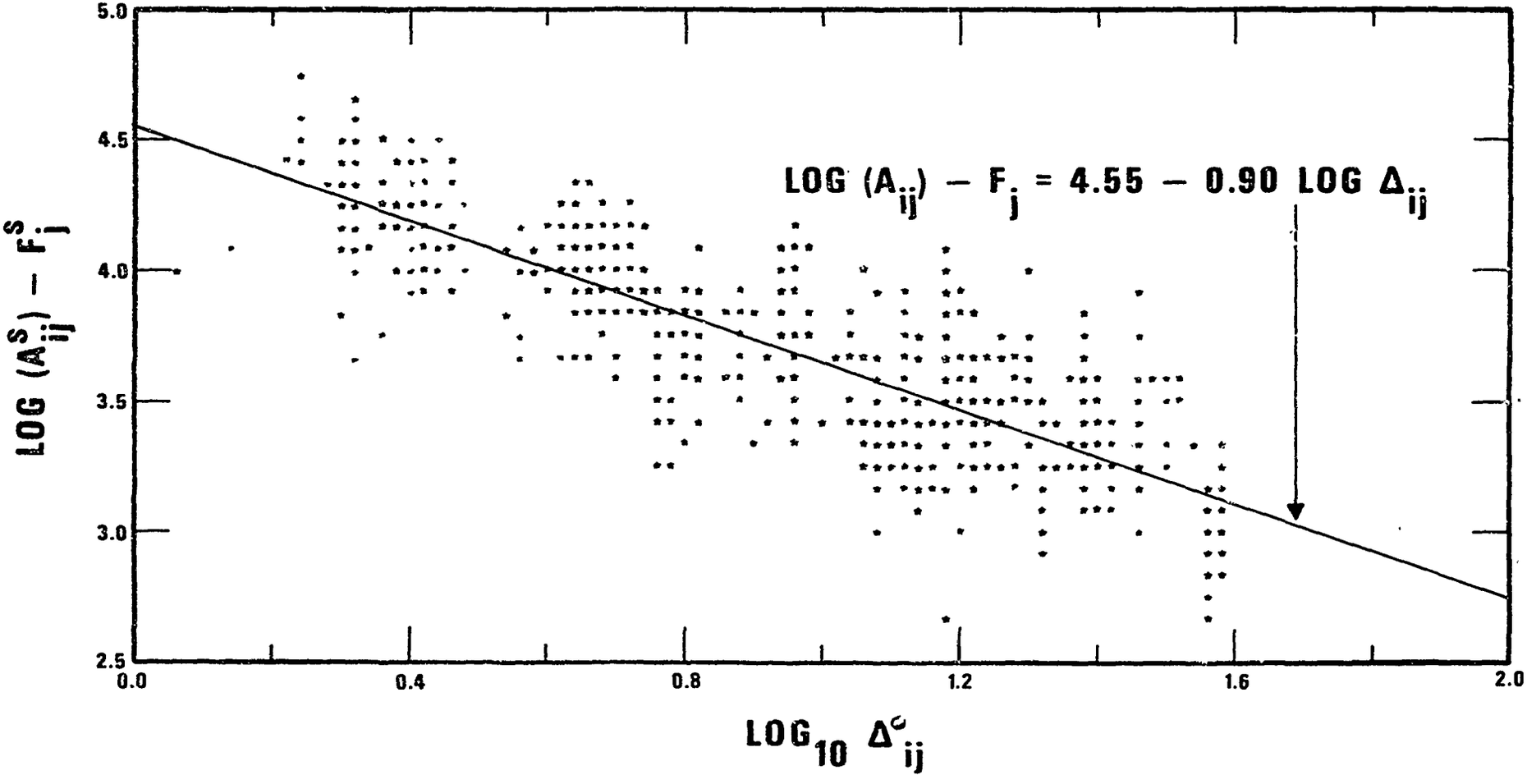

Figure 1a. Logarithms of observed amplitudes minus event terms (A_{ij} - F_j) versus log-distance for Rayleigh waves from NTS explosions to North America stations.

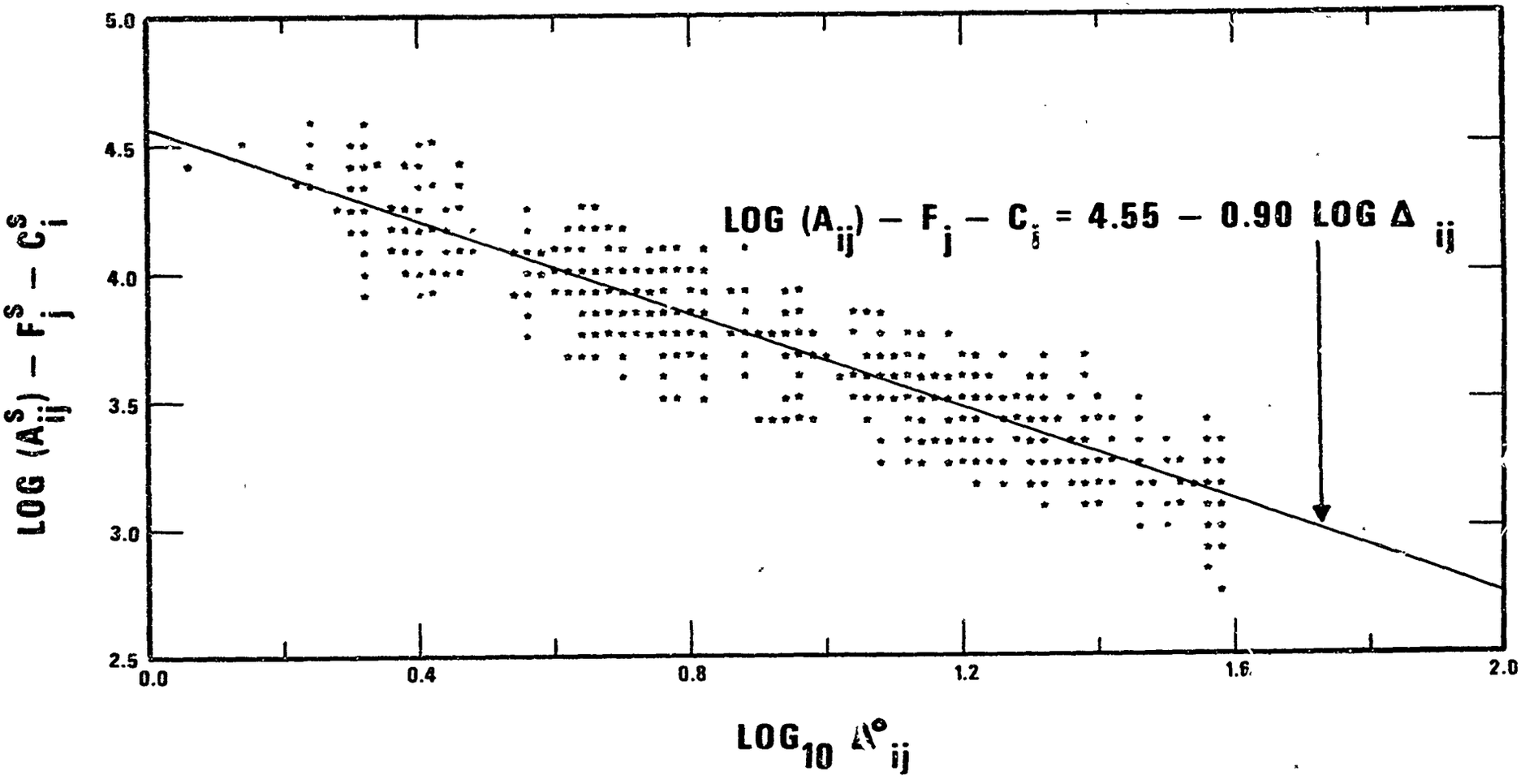

Figure 1b. Same data as Figure 1a, but with station terms, C_i, subtracted.

seconds and by assuming that the maximum amplitude on the recording is an Airy phase at teleseismic distances.

Linear amplitude-distance functions were determined using the final 664 readings after the data were converted to $\bar{A}$ and A/T using the reported periods. The results are summarized in Table III for comparison with the amplitude-distance function using A. Since the confidence interval is proportional to the standard deviation of the data, Table III shows that A and $\bar{A}$ are as good as or better measures than A/T, in a statistical sense, when estimating magnitudes.

Compressional-wave data

Essentially the same procedure was followed with the compressional-wave data for the 79 NTS events. Before any processing, all stations outside of the North American continent were deleted. Event SHREW, with one probably spurious reading, was discarded. In addition, since there were many more stations having recorded P waves than LR waves, it was decided to retain only those stations in this analysis which had at least three compressional-wave readings. Several hundred observations were discarded in this way. After all these deletions, there remained 1474 readings from 106 stations for 78 events.

Magnitude was then calculated for each observation in the routine manner, using Evernden's (1967) regional correction formulas in conjunction with Gutenberg and Richter's (1956) correction factors for teleseismic

TABLE III

M_s and m_b Formulas Using Various Measures of Amplitude

	M_s		m_b	
Measure	Distance Relation	95% CI on Slope	Distance Relation	95% CI on Slope
A	$\log A = 4.55 - 0.900 \log\Delta$	.027	$\log A = 2.11 - 0.870 \log\Delta$	.033
$\overline{A}$	$\log A = 3.99 - 0.716 \log\Delta$	.028	$\log\overline{A} = 2.16 - 0.608 \log\Delta$	.028
$\frac{A}{T}$	$\log\frac{A}{T} = 3.48 - 0.967 \log\Delta$	.032	$\log\frac{A}{T} = 2.55 - 1.150 \log\Delta$	.028

distances. In order to eliminate possibly erroneous data, as for the Rayleigh waves, all readings which resulted in a station magnitude deviating more than one unit from the event average were discarded. A total of 75 readings were discarded in this way, and four more were discarded because two stations were left with only two readings each. Program JMD was run on these remaining data. Normality of the magnitude residual distribution was again assumed, with a calculated 0.22 standard deviation; and all measurements giving a value of $(\hat{F}_{ij} - \hat{F}_j)$ greater than approximately two standard deviations of the $\hat{F}_{ij}$'s ($\pm$ 0.45 was actually used) were discarded. This comprised 34 measurements, and two more were discarded when one station had only two readings left. JMD was repeated on the remaining data, and only three readings failed to meet the $\pm$ 0.45 criterion. In all, approximately 8 per cent of the data were discarded because they were anomalous and possibly erroneous. Using the 1356 remaining readings, the final run of JMD resulted in values for $\hat{B}$ and $\hat{H}$ of 0.87 and 2.11 respectively, with $\pm$ 0.03 95 per cent confidence limits on the slope $\hat{B}$. The final even+ terms (equivalent to m_b) are given in Table IV , and the final station terms in Table V. Thus, for compressional waves from NTS to North American stations we have this unified distance relation by substituting the above calculated values of slope and intercept into the original model:

$$\log A_{ij} = 2.11 - 0.87 \log r_{ij} + \hat{F}_j + \hat{C}_i$$

where A is in millimicrons (zero-to-peak) and r is in

TABLE IV

Compressional-Wave Event Terms

EVENT	F	NUMBER OF STATIONS
*AARDVARK	.43	23
*ACUSHI	- .63	11
*AGOUTI	- .69	17
*ALLEGHENY	-1.00	9
*ANTLER	- .28	5
*ARMADILLO	- .45	23
AUK	.15	28
BENHAM	1.73	7
BILBY	1.08	30
*BOBAC	- .67	14
BOURBON	.31	14
BOXCAR	1.72	12
BRONZE	.48	29
BUFF	.52	20
*CASSELMAN	- .58	14
CHARCOAL	.33	19
CHARTREUSE	.73	18
*CHENA	-1.21	7
*CHINCHILLA	-1.05	17
*CHINCHILLA2	-1.42	10
*CIMARRON	- .20	23
*CLEARWATER	.42	17
*CODSAW	- .94	17
COMMODORE	1.13	16
CORDUROY	1.06	21
CUP	.47	29
*DESMOINES	- .57	9
DILUTED WATERS	- .29	20
*DOORMOUSE	- .61	22
*DOORMOUSE PRIME	- .49	21
DUMONT	.94	21
DURYEA	.49	20
*FEATHER	-1.79	6
*FISHER	- .71	16
FORE	.48	34
GREELEY	1.75	15
HARDHAT	- .02	23
HAYMAKER	.15	26
HALFBEAK	1.51	16
*HYRAX	- .64	15
*KAWEAH	-1.00	14
KLICKETAT	.26	26
KNICKERBOCKER	.66	13
*MAD	-1.77	5
*MADISON	- .44	16
MARSHMALLOW	- .28	16
MERRIMEC	- .52	14
*MINK	-1.30	6
MISSISSIPPI	.52	27
NASH	.52	15
*PACKRAT	- .59	16
PALANQUIN	- .66	17
*PAMPAS	- .59	18
*PAR	.01	26
*PASSAIC	- .53	21
*PEBA	- .48	19
PILEDRIVER	.98	20
PINSTRIPE	- .15	11
*REDHOT	-1.01	9
REX	.16	19
*RINGTAIL	-1.09	12
*ROANOKE	-1.12	9
*SACRAMENTO	- .80	8
*SANTEE	- .78	17
SCOTCH	1.11	16
SCROLL	- .48	12
*SEDAN	- .17	13
*STILLWATER	- .65	17
*STOAT	- .91	16
*STONES	.27	20
*STUTZ	- .29	17
TAN	.97	21
TURF	.19	30
WAGTAIL	.62	25
*WICHITA	- .74	14
WISHBONE	- .30	19
*YORK	- .45	22
*YUBA	- .61	21

* Not used in M_s vs m_b fit.

degrees. Figures 2a and 2b show for compressional waves, as Figures 1a and 1b did for Rayleigh waves, that the addition of station terms reduces the scatter. Figure 2a is typical of the variation of body-wave amplitude versus distance plots, in that amplitude is not a smooth or simple function of distance. This character is due to the fact that various branches of the travel-time curve contribute first arrivals out to around 20° distance and that ray paths to various distances sample widely changing Q properties of the mantle. Certainly the straight-line approximation calculated here is not a good fit to the data; but, as Figure 2b shows, when this approximation is used in conjunction with station terms which are operating somewhat as distance-correction terms, a small scatter in station magnitudes for any given event should result.

The statistical stability of the two other measures, $\bar{A}$ and A/T, were assessed after converting A to these measures using the reported periods. The JMD program was run with the final 1356 observations used for the A versus distance fit. Table III compares these results, and the confidence limits on the slope show that all three of these measures for compressional waves have approximately the same statistical stability. The A/T measure, however, does show somewhat less variance for m_b than A, whereas the reverse is true for M_s. Gutenberg (1945) stated that his body-wave amplitudes were more consistent when divided by the observed period, and the A/T measure became routine for m_b calculations thereafter.

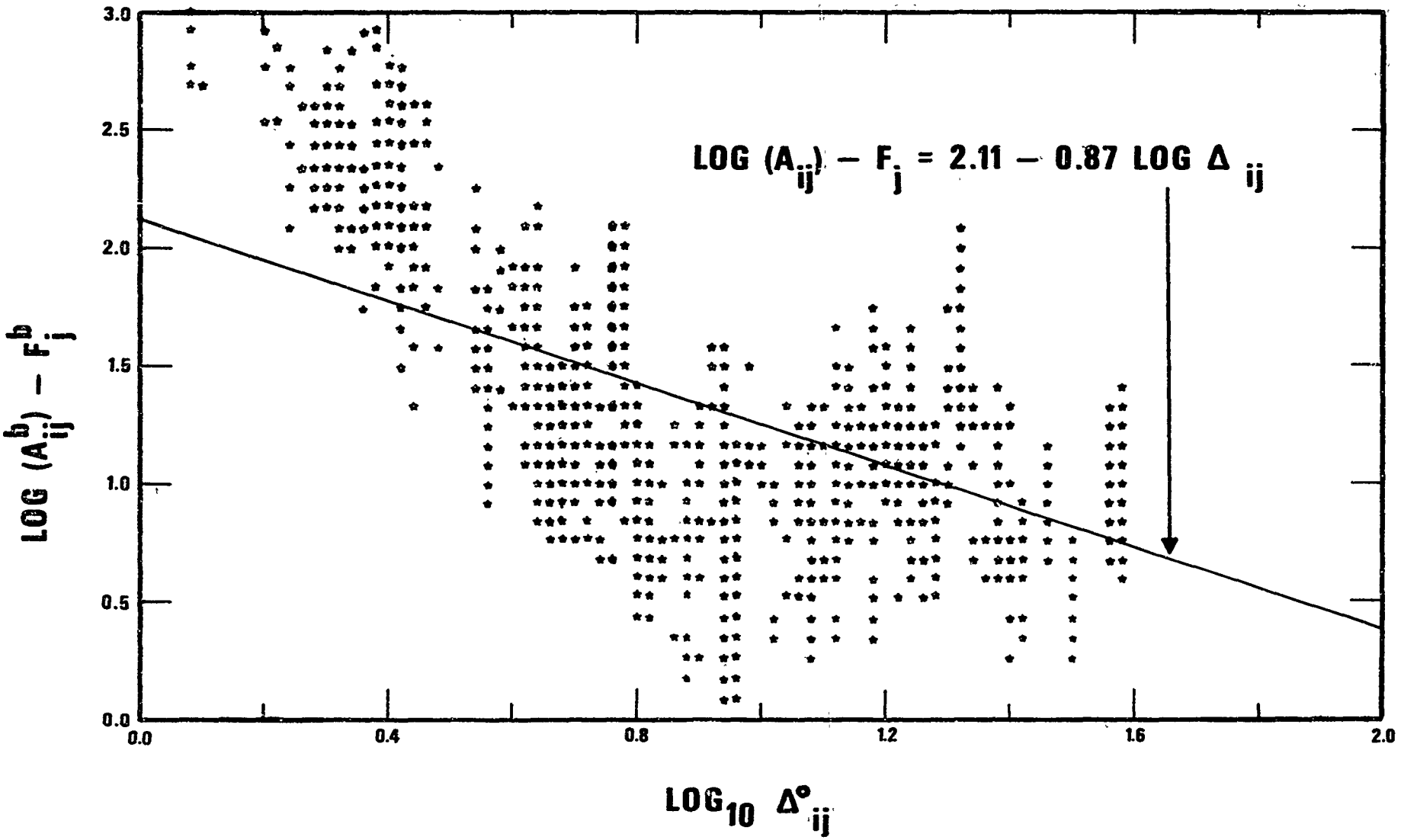

Figure 2a. Logarithms of observed amplitudes minus event terms (A_{ij} - F_j) versus log-distance for compressional waves from NTS explosions to North America stations.

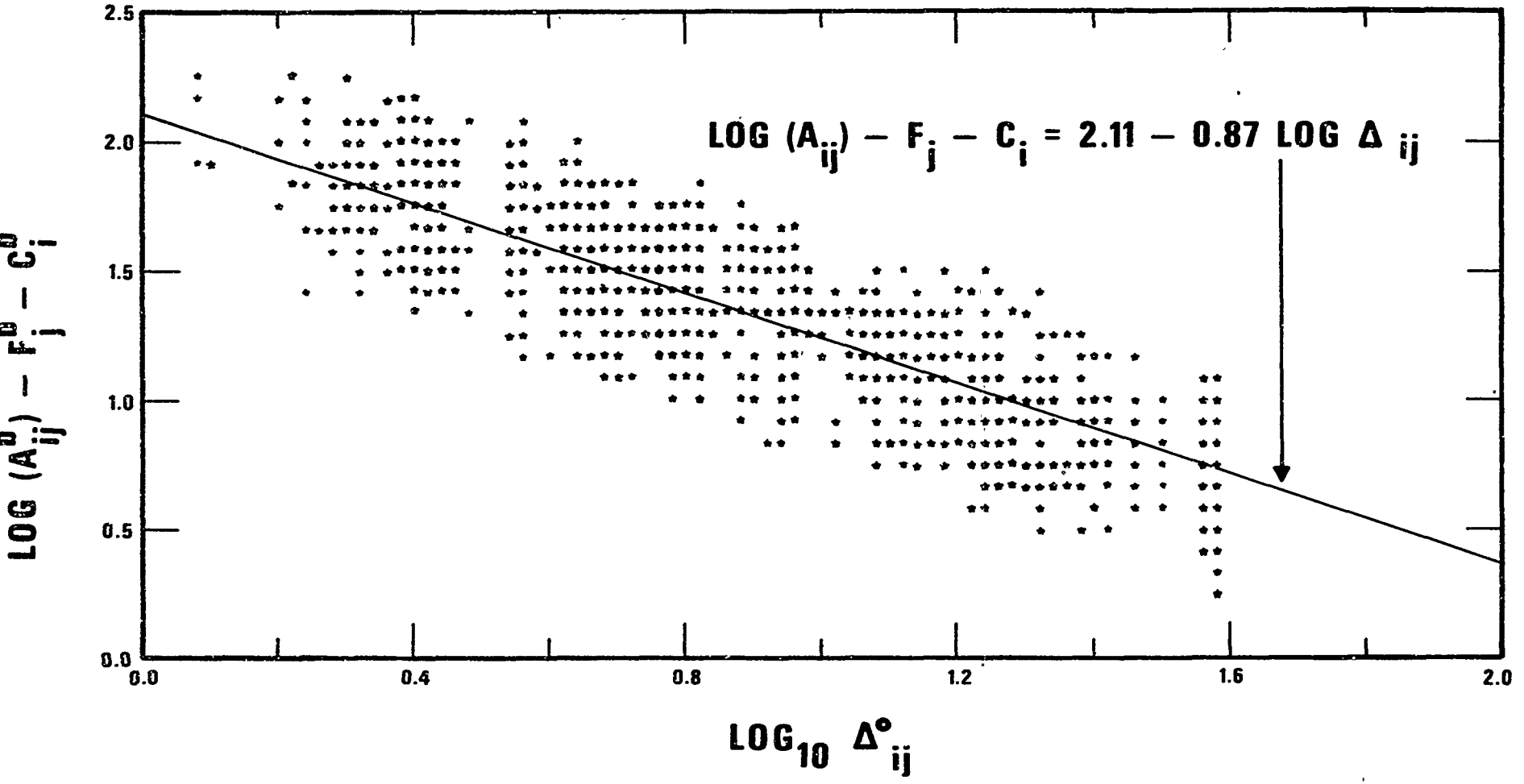

Figure 2b. Same data as Figure 2a, but with station terms, C_i, subtracted.

Distribution of magnitude residuals and correlation of station terms

Recall that we assumed a normal distribution for both the compressional-wave and Rayleigh-wave magnitude residuals $(\hat{F}_{ij} - \hat{F}_j)$. We plot in Figure 3 the histograms of the residuals, using the final 664 and 1356 readings. Both distributions appear to be normal. Since the data were truncated beyond approximately two standard deviations from the mean, a slight modification of the Smirnov-Kolmogorov test for normality was made before it was applied to this data. The compressional-wave residuals passed the normality test at well above a 0.2 level of acceptance, while the surface-wave residuals passed at only a 0.05 level of acceptance. (Levels were taken from Lilliefors, 1967.) The isolated peak around the mean of the surface-wave residuals in Figure 3 undoubtedly accounts for this low level of acceptance. If the magnitude is regarded as normally distributed, then amplitudes must have a log-normal distribution. This log-normal behavior has been found for two short-period data sets entirely different than the NTS one considered here. Freedman (1967) found WWNSS observations to have this distribution, and Klappenberger (1967) showed that LASA sub-array amplitudes for individual events had this distribution.

We checked the correlation of Rayleigh-wave and compressional-wave station terms at those stations which appear in both Table II and V. The correlation coefficient was -0.10, which indicates that the two groups of station terms are highly uncorrelated.

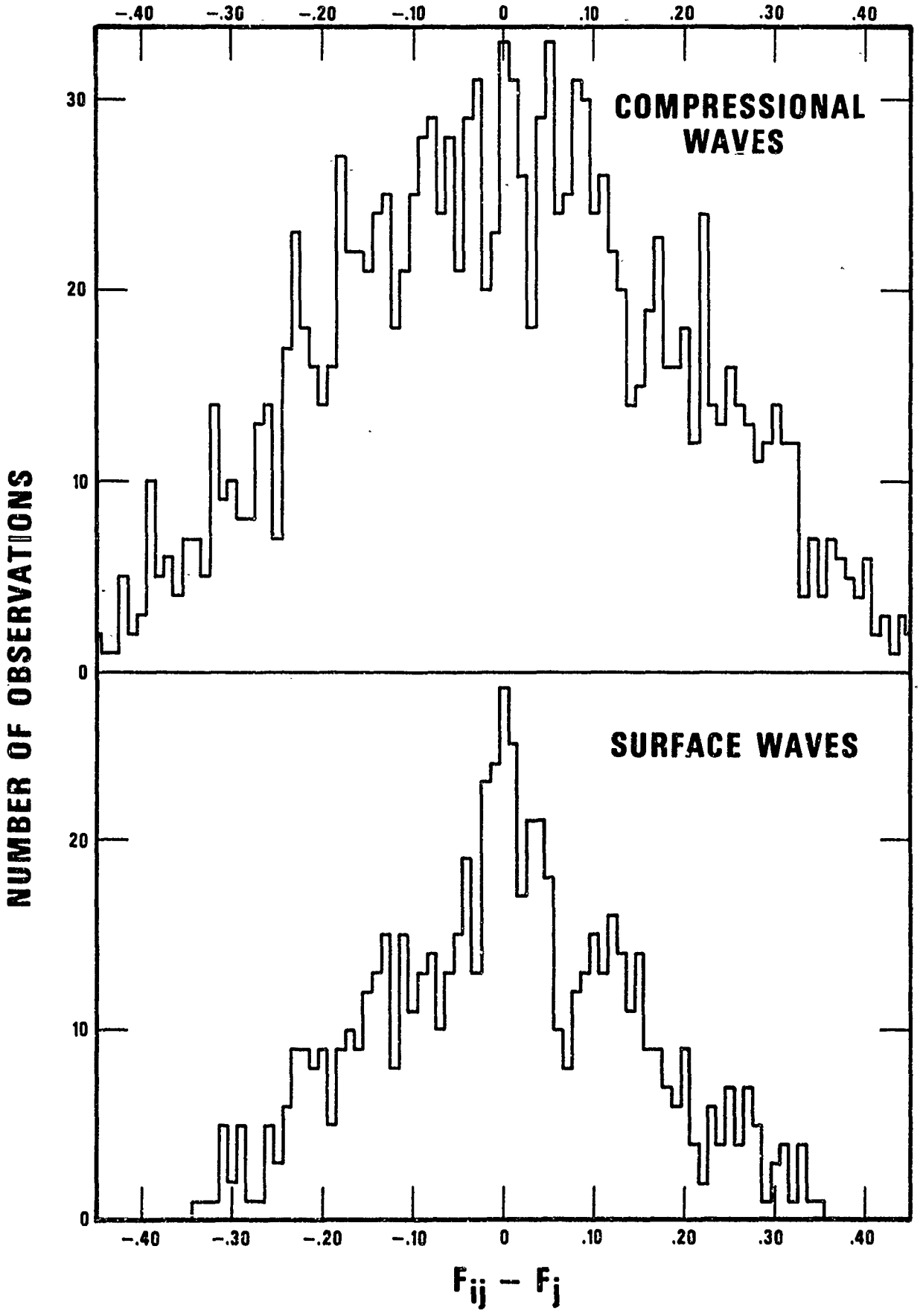

Figure 3. Distributions of (F_{ij} - F_j) for compressional and surface waves.

TABLE V

Compressional-Wave Station Terms

STATION	C	NUMBER OF EVENTS	STATION	C	NUMBER OF EVENTS
AN-MA	-.12	3	KN-UT	.57	72
AP-OK	.31	4	LAO	-.55	13
AR-WS	.40	4	LC-NM	-.80	34
AT-NV	.75	16	LG-AZ	-.10	10
AX2AL	.33	10	LP-TX	-.14	5
BE-FL	.19	7	MC-SD	.04	3
BF-CL	.64	12	ML-NM	-.65	6
BL-WV	-.15	13	MM-TN	-.04	7
BMO	-.79	30	MN-NV	.62	75
BM-TX	-.03	3	MO-ID	-.36	5
BP-CL	.64	3	MP-AR	-.01	14
BR-PA	.04	8	MV-CL	-.37	34
BX-UT	-.13	3	ND-CL	-.14	4
CG-VA	.12	3	NG-WS	.04	6
CK-BC	-.11	4	NL2AZ	-.09	10
CN-WS	.36	4	NP-NT	.34	27
CPO	.06	31	PG-BC	-.06	16
CP-CL	.12	41	PI-WY	-.17	5
CR-NB	.23	9	PM-WY	-.52	16
CT-OK	-.06	4	PT-OR	.02	25
CU-NV	.73	4	RG-SD	-.38	8
DH-NY	-.28	10	RK-ON	.70	28
DR-CO	-.44	37	RT-NM	-1.23	7
DU-OK	.40	4	RY-ND	.63	4
DV-CL	.77	5	SE-MN	.19	17
EB-MT	-.02	5	SF-AZ	.07	13
EF-TX	-.48	6	SG-AZ	.16	8
EK-NV	.52	5	SI-BC	-.18	10
EN-MO	-.04	3	SJ-TX	.40	6
EU-AL	-.06	3	SK-TX	.02	4
EY-NV	.24	5	SN-AZ	-.13	10
FK-CO	-.20	6	SS-TX	-.38	15
FM-UT	-.32	36	ST-NV	.24	3
FO-TX	-.57	4	SV-AZ	-.28	4
FR-MA	-.02	5	SV3QB	.21	23
FS-AZ	.19	37	SW-MA	-.04	10
GE-AZ	-.56	10	TC-NM	-.35	10
GI-MA	-.08	5	TFO	-.32	37
GV-TX	.17	6	TF-CL	-.24	15
HB-OK	.14	6	TK-WA	-.48	5
HE-TX	.43	4	TN-CL	.29	11
HK-WY	-.17	4	TS-ND	-.24	3
HL-ID	-.64	49	UBO	.35	35
HN-ME	.29	27	VN-UT	.22	12
HR-AZ	-.37	8	VT-OR	-.11	11
HY-MA	-.62	3	WH2YK	-.35	8
JE-LA	.42	3	WI-NV	-.10	42
JP-AT	-.46	8	WMO	-.01	30
JR-AZ	.17	10	WM-AZ	.20	15
KC-MO	.15	9	WN-SD	.16	9
KG-AZ	.51	4	WO-AZ	-.48	9
KM-CL	.33	4			

Ericsson (1971) has obtained the same result with magnitudes from Canadian stations for NTS explosions. Since our $\hat{C}_i$'s operate somewhat as distance-effect terms, the interpretation of the correlation coefficient is tenuous; and if compressional-wave station terms had been calculated relative to a curve or to line segments which more closely fit the actual amplitude-distance data, the correlation coefficient might well have been higher.

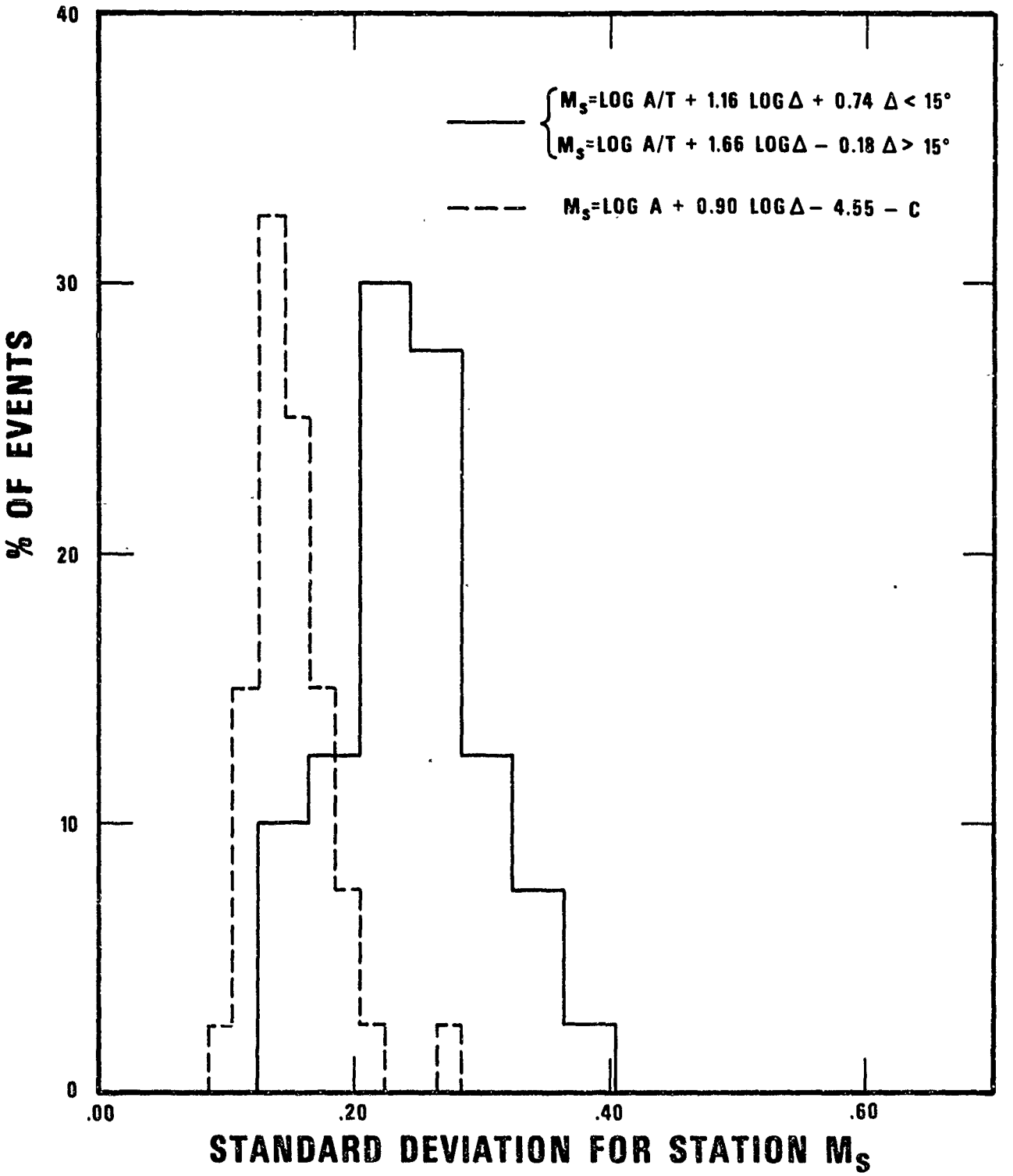

Figure 4a. Histograms of standard deviations of M_S estimates for 41 NTS events using JMD and conventional methods.

standard deviations for 78 explosions are calculated from JMD and conventional m_b estimates with the same data base (all of the events of Table IV were used). The conventional estimates are made using Evernden's (1967) distance-correction formulas for the Western United States and Gutenberg and Richter's (1956) teleseismic distance-correction terms. Again the reduction in variance is due to the inclusion of station terms in the JMD estimation. Ericsson (1971) shows nearly identical results using Canadian magnitudes for NTS explosions. This approximately 100 per cent reduction in variance for M_s and m_b station estimates should, as Ericsson points out, correspondingly reduce the scatter of the M_s vs m_b plot using network averages. To test this, we took 36 of the 43 explosions in Table I. FISHER, MADISON, PAMPAS, REDHOT, and STUTZ were not used because, with three or less observations, their M_s was not well estimated. SEDAN was eliminated since it was actually a cratering event and appears anomalous on any M_s vs m_b plot. PAR was eliminated because it has appeared highly anomalous on preliminary M_s vs m_b plots (Lambert, 1971), but we have no explanation for this anomaly. The Rayleigh-wave event terms from Table I and corresponding compressional-wave event terms from Table IV were used in a least-squares program which fits a straight line to data. Note that since the slope is nearly one for the fitted lines, the regression of m_b on M_s could not differ significantly from that of M_s on m_b and also the variance of m_b and M_s about the fitted line would be nearly equal. Here and in all subsequent least-squares fits the points were equally

weighted. The program was also employed to fit the "adjusted" M_s vs m_b data for these same 36 events, as given in Lambert (1971). Using the truncated data sets of this report (664 observations for Rayleigh waves and 1356 observations for compressional waves) the event magnitudes were computed using the routine formulas just as Lambert did; and the resulting revised M_s and m_b for the events are listed in Table VI. The values differ slightly, or not at all, from those taken from Lambert; and they were also fitted with a straight line. The fitting results are listed in Table VII for the three cases; and the actual data points with the least-squares lines are shown in Figures 5, 6, and 7 for Lambert's values, revised Lambert's values, and JMD values, respectively. The variances about the lines listed in Table VII show that some difference in scatter for the three plots exists. Little decrease in variance was obtained by using magnitudes estimated from the truncated data, which comprised about 93% of the full data set used by Lambert. Since the truncation merely removed tails from both sides of the distribution, leaving means essentially unchanged as indicated by Table VI, little or no improvement was to be expected. The use of JMD results versus routine magnitude estimation did not decrease the variance of the average M_s vs m_b points, and this is somewhat surprising in view of the approximate fourfold decrease of the variance of station M_s and m_b estimates as shown by Figures 4a and 4b when JMD is employed.

We have not yet shown how much JMD magnitude

TABLE VI

Comparions of Average Magnitudes for 36 NTS Explosions When Full Data Set (Lambert) and Truncated Data Set (Revised) are used with Routine Magnitude Formulas.

	M_s		m_b	
EVENT	LAMBERT	REVISED	LAMBERT	REVISED
AUK	3.97	3.92	4.50	4.48
BENHAM	5.72	5.79	5.89	6.28
BILBY	5.12	5.12	5.48	5.45
BOURBON	4.49	4.52	4.78	4.77
BOXCAR	5.86	5.95	6.14	6.34
BRONZE	4.50	4.51	4.87	4.86
BUFF	4.21	4.22	4.87	4.86
CHARCOAL	4.00	4.00	4.82	4.82
CHARTREUSE	4.33	4.33	5.04	5.12
COMMODORE	5.24	5.24	5.40	5.54
CORDUROY	4.77	4.77	5.42	5.40
CUP	4.30	4.29	4.84	4.83
DILUTED WATERS	3.46	3.50	4.05	4.05
DUMONT	4.69	4.69	5.27	5.32
DURYEA	4.25	4.21	4.82	4.83
FORE	4.11	4.09	4.80	4.77
GREELEY	5.79	5.83	6.13	6.17
HARDHAT	*3.74	3.72	4.43	4.34
HAYMAKER	3.98	3.98	4.34	4.40
HALFBEAK	5.39	5.36	5.78	5.93
KLICKETAT	4.04	4.04	4.57	4.52
KNICKERBOCKER	4.78	4.79	5.22	5.13
MARSHMALLOW	3.39	3.27	4.01	4.02
MERRIMEC	3.45	3.45	3.73	3.78
MISSISSIPPI	4.02	3.99	4.70	4.75
NASH	4.14	4.26	4.93	4.93
PALANQUIN	3.26	3.26	3.75	3.76
PILEDRIVER	4.47	4.47	5.32	5.33
PINSTRIPE	3.53	3.49	4.09	4.11
REX	4.27	4.26	4.52	4.55
SCOTCH	5.21	5.18	5.39	5.58
SCROLL	3.06	3.26	3.89	3.90
TAN	4.48	4.49	5.30	5.28
TURF	4.06	4.05	4.55	4.52
WAGTAIL	4.26	4.26	5.03	5.04
WISHBONE	3.38	3.42	3.97	4.01

*This value differs from that (3.88) reported by Lambert (1971), who did not use all the available data. This value would have resulted had he done so.

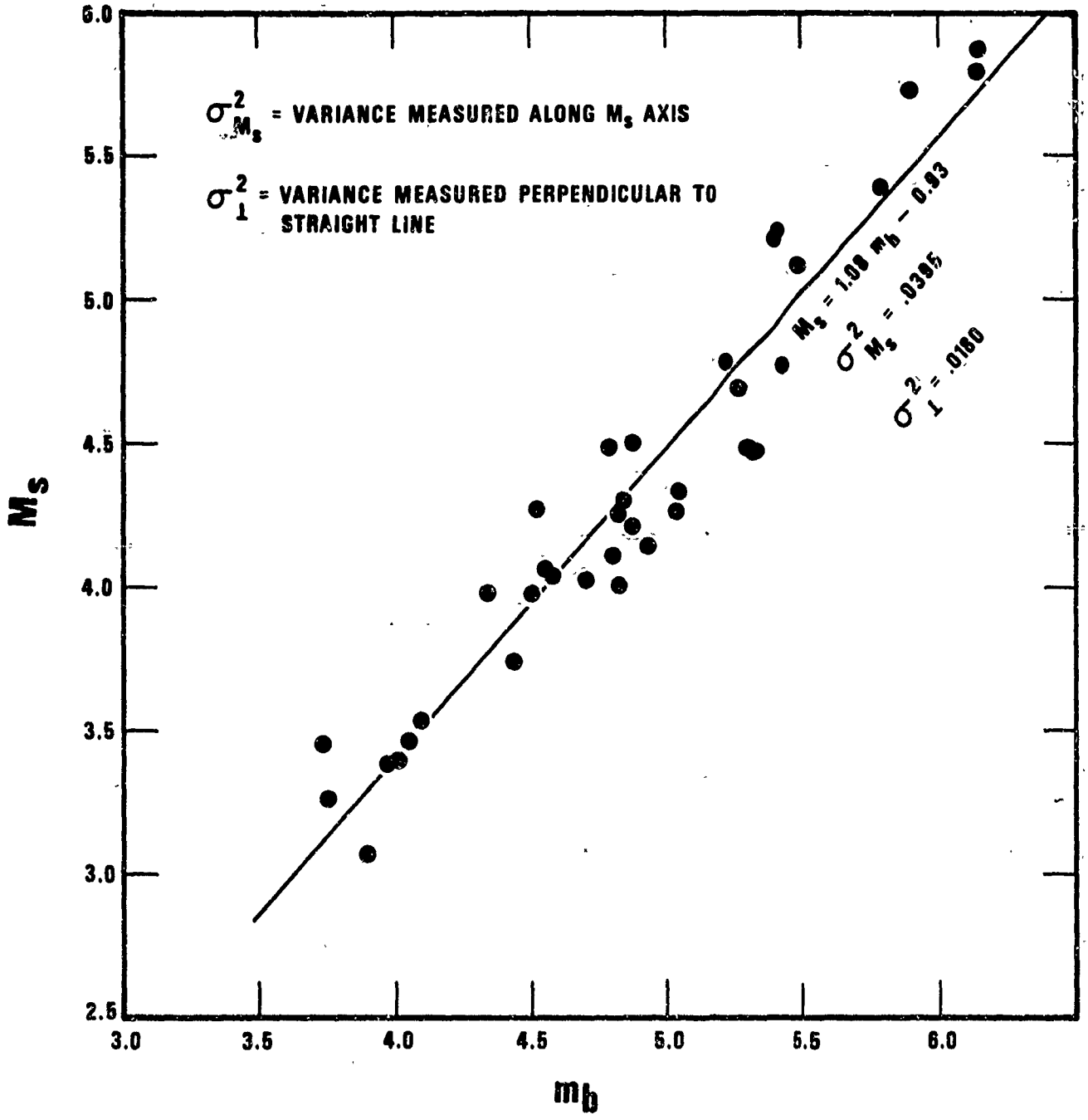

Figure 5. M_S vs m_b of 36 NTS events using routine magnitude estimation -- from Lambert (1971).

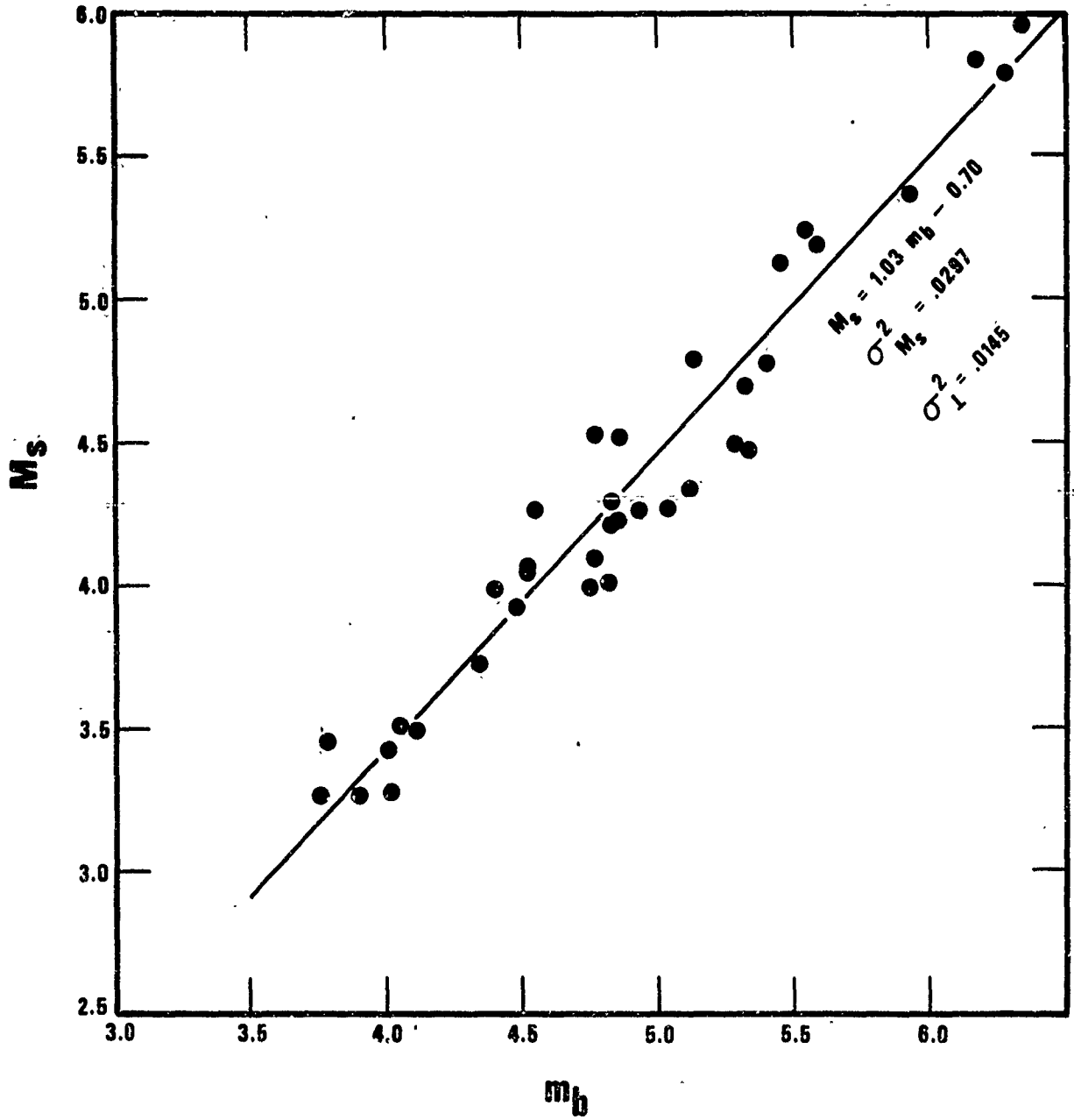

Figure 6. M_S vs m_b of 36 NTS events using routine magnitude estimation with the truncated data sets of this report.

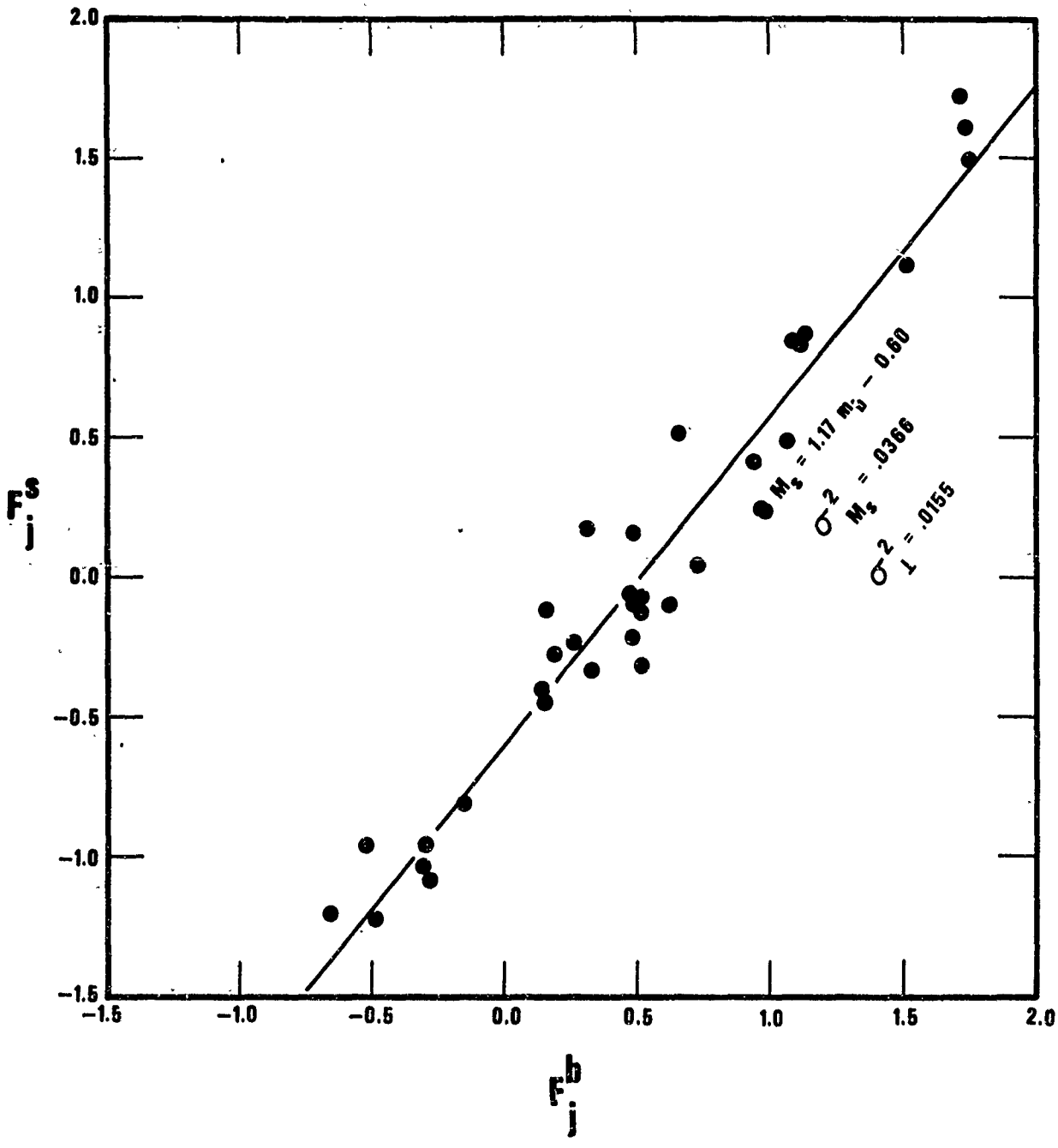

Figure 7. M_S vs m_b of 36 NTS events using JMD results with A measure.

TABLE VII

M_s vs m_b Relations Using Various Means of Magnitude Estimation for 36 NTS Events

ESTIMATION PROCEDURE	M_s vs m_b RELATION	VARIANCE OF M_s ABOUT THE PREDICTED RELATION
Routine (Lambert's original)	$M_s = 1.08\ m_b - 0.93$	.0395
Routine (Lambert's revised)	$M_s = 1.03\ m_b - 0.70$	.0297
JMD(A)	$M_s = 1.17\ m_b - 0.60$	.0366
JMD($\overline{A}$)	$M_s = 1.41\ m_b - 0.65$	.0321
JMD(A/T)	$M_s = 1.19\ m_b - 0.57$	.0337

estimates differed from those made with routine formulas. To do this, we must first raise the 36 event terms F to a level equivalent to our routine M_s and m_b values. We will add to the event terms a term R given by

$$R_s = \frac{1}{36} \sum_{j=1}^{36} (M_s - \hat{F})_j$$

for surface-wave magnitudes and by

$$R_b = \frac{1}{36} \sum_{j=1}^{36} (m_b - \hat{F})_j$$

for body-wave magnitudes, where M_s and m_b refer to the revised values given in Table VI and $\hat{F}$ refers to the JMD event terms of Tables I and IV. The calculated value of R_s was 4.34; that of R_b was 4.39. We list in Table VIII the differences in routine and JMD magnitude estimates after these normalizing R terms are added to the event terms $\hat{F}$. It is evident that, regardless of the fourfold decrease of station magnitude variance with JMD due to station terms, the JMD average event magnitudes have changed very little from conventional ones. This seems to account for the failure of JMD to provide a M_s vs m_b plot with less scatter. We must conclude at this point that the observed M_s vs m_b points in Figures 5 and 6 are real and relatively unbiased by the particular network recording each event. Since JMD results in Figure 7 fail to reduce the scatter, we must

TABLE VIII

Difference Between Magnitudes Computed Routinely and by JMD For 36 NTS Events

EVENT	ROUTINE - JMD ESTIMATION M_s-F^s	m_b-F^b
AUK	.03	-.06
BENHAM	-.15	.16
BILBY	-.06	-.02
BOURBON	.01	.07
BOXCAR	-.10	.23
BRONZE	.02	-.01
BUFF	-.04	-.05
CHARCOAL	.00	.10
CHARTREUSE	-.05	.00
COMMODORE	.04	.02
CORDUROY	-.05	-.05
CUP	.02	-.03
DILUTED WATERS	.12	-.05
DUMONT	-.06	-.01
DURYEA	-.03	-.05
FORE	-.03	-.10
GREELEY	.00	.03
HARDHAT	.01	-.03
HAYMAKER	.05	-.14
HALFBEAK	-.09	.03
KLICKETAT	-.06	-.13
KNICKERBOCKER	-.06	.08
MARSHMALLOW	.02	-.09
MERRIMEC	.07	-.09
MISSISSIPPI	-.03	-.16
NASH	.05	.02
PALANQUIN	.13	.03
PILEDRIVER	-.10	-.04
PINSTRIPE	-.03	-.13
REX	.04	.00
SCOTCH	.01	.08
SCROLL	.15	-.01
TAN	-.09	-.08
TURF	-.01	-.06
WAGTAIL	.02	.03
WISHBONE	.12	.08

accept such scatter and attribute it to differences in source parameters rather than notwork biases. These parameters are source depth, medium (including density, rigidity, bulk modulus, porosity, water content, etc.), and relative tectonic component; but it is beyond the scope of this report to relate these to observed magnitudes.

Finally, we use the JMD results with the $\overline{A}$ and A/T measure as discussed earlier to construct M_s vs m_b plots in Figures 8 and 9 respectively. The actual F terms are given in Table IX. Straight-line fits were made to these data, and the results are listed in Table VII along with the other M_s vs m_b lines. Calculated variances indicate that the scatter of these last two plots is somewhat less than the previous one where A was used as the measure, but whether this is significantly less is questionable.

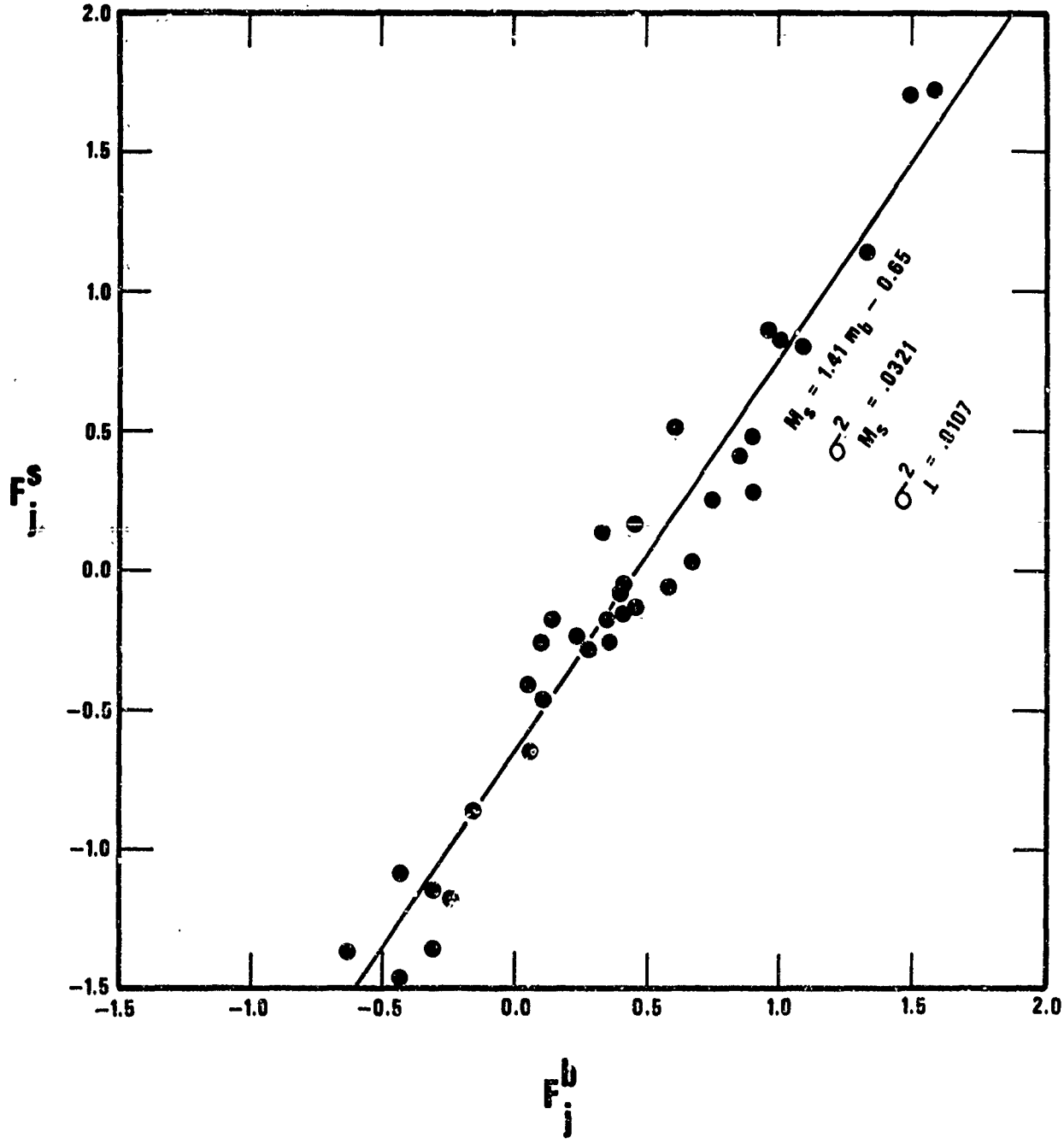

Figure 8. M_s vs m_b of 36 NTS events using JMD results with $\overline{A}$ measure.

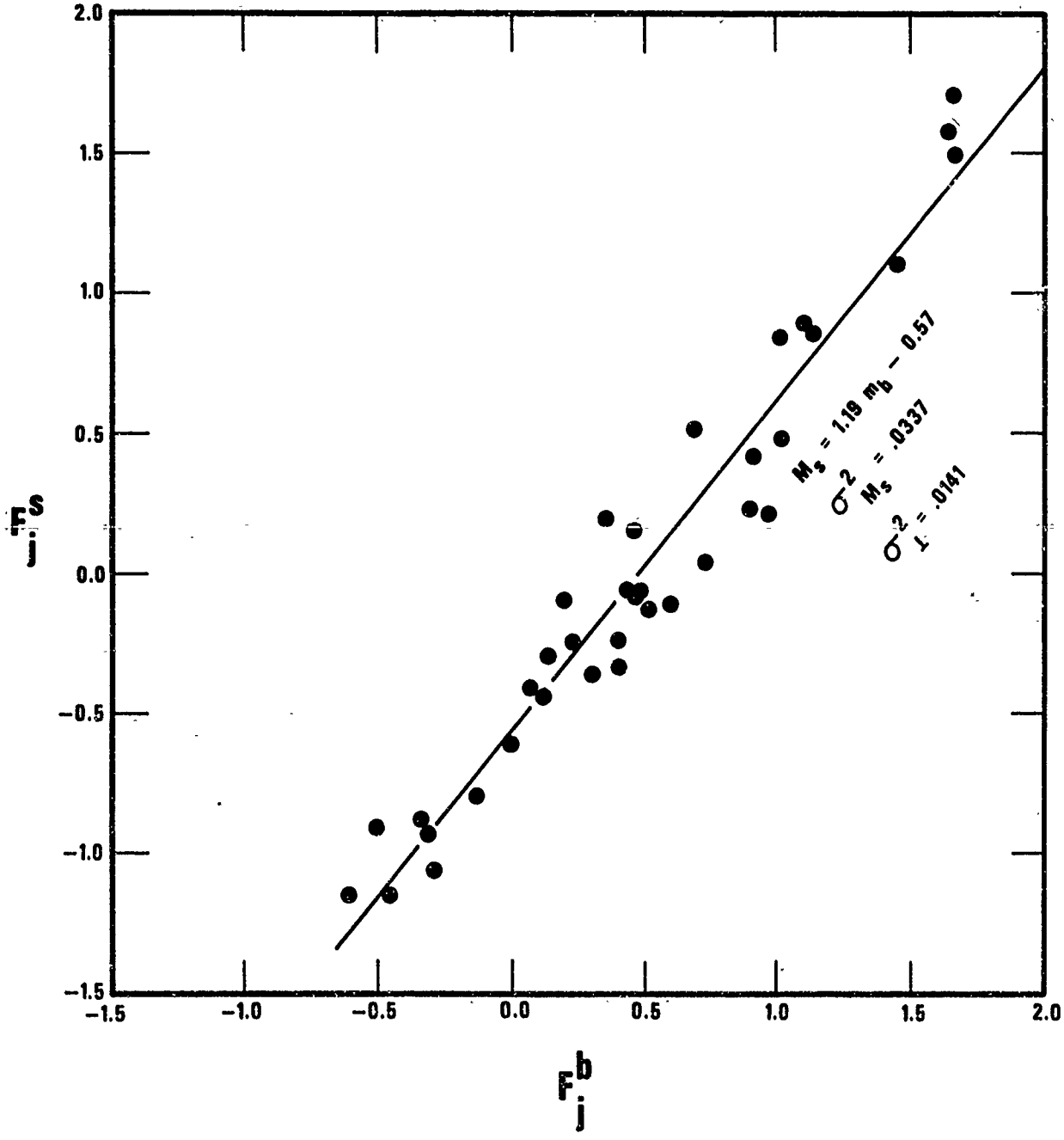

Figure 9. M_S vs m_b of 36 NTS events using JMD results with A/T measure.

TABLE IX

Event Terms From JMD Using $\bar{A}$ and A/T Measures

EVENT	F^s $\bar{A}$	F^s A/T	F^b $\bar{A}$	F^b A/T
AUK	-.46	.44	.11	.12
BENHAM	1.70	1.57	1.49	1.64
BILBY	.86	.84	.96	1.01
BOURBON	.14	.19	.33	.36
BOXCAR	1.72	1.70	1.58	1.66
BRONZE	.16	.15	.46	.46
BUFF	- .08	- .08	.40	.47
CHARCOAL	- .29	- .36	.28	.30
CHARTREUSE	.03	.04	.67	.73
COMMODORE	.82	.88	1.00	1.10
CORDUROY	.48	.48	.90	1.02
CUP	- .05	- .07	.42	.43
DILUTED WATERS	-1.15	- .88	- .31	- .33
DUMONT	.41	.41	.85	.91
DURYEA	- .16	- .07	.41	.48
FORE	- .18	- .24	.35	.40
GREELEY	1.50	1.40	1.50	1.67
HARDHAT	- .65	- .61	.06	.00
HAYMAKER	- .41	- .41	.05	.07
HALFBEAK	1.14	1.10	1.33	1.45
KLICKETAT	- .23	- .25	.23	.23
KNICKERBOCKER	.51	.51	.61	.68
MARSHMALLOW	-1.18	-1.06	- .24	- .29
MERRIMEC	-1.09	- .91	- .43	- .51
MISSISSIPPI	- .26	- .34	.36	.40
NASH	- .13	- .13	.46	.52
PALANQUIN	-1.37	-1.15	- .63	- .61
PILEDRIVER	.28	.21	.90	.97
PINSTRIPE	- .87	- .80	- .16	- .13
REX	- .17	- .10	.14	.20
SCOTCH	.80	.85	1.08	1.13
SCROLL	-1.47	-1.15	- .43	- .46
TAN	.25	.23	.75	.90
TURF	- .26	- .30	.10	.14
WAGTAIL	- .06	- .12	.58	.60
WISHBONE	-1.36	.93	- .31	- .31

ANALYSIS OF SCATTER IN M_s vs m_b PLOTS

We desire to show how the foregoing results fit into an amplified statistical discussion of M_s and m_b. The statistical model and stated results in this section closely parallel the work of Ericsson (1971). One important distinction is that he used known yields to estimate the variance of the error terms in the model whereas we ignore yield information and obtain nearly identical results from the seismic measurements themselves. Also we employ a significantly larger set of explosions (36) in the analysis of variance than Ericsson, who used only six. We will compare the variance of single-station M_s vs m_b plots with network M_s vs m_b plots because this has practical importance and was not discussed by Ericsson.

First we take each station's calculated magnitude for a given event to be given by equation (10). Then we consider Z_{ij} to be composed of the predicted log-amplitude term $\hat{X}_{ij}$ plus a random normal error term $\hat{E}_{ij}$ peculiar to that station-event pair as indicated by equation (1). Thus

$$\hat{F}_{ij} = \hat{X}_{ij} + \hat{BR}_{ij} - \hat{H} - \hat{C}_i + \hat{E}_{ij} \tag{11a}$$

when station corrections are included; or

$$\hat{F}'_{ij} = \hat{X}_{ij} + \hat{BR}_{ij} - \hat{H} + \hat{E}_{ij} \tag{11b}$$

when they are not. The prime henceforth denotes an estimate made without the use of station terms $\hat{C}_i$. $\hat{E}_{ij}$ is

"measurement noise" introduced by seismic background on the recordings, by calibration errors, and by the analyst's subjective measurement of amplitude and period of the maximum excursion. $\hat{C}_i$ is "path station noise" which is due to varying propagation and site factors and inability of a single straight line to fit the amplitude-distance data as well as line segments or polynomials. Applying the definition of $\hat{X}_{ij}$ to (11a) and (11b), we obtain simply:

$$\hat{F}_{ij} = \hat{F}_j + \hat{E}_{ij} \tag{12a}$$

$$\hat{F}'_{ij} = \hat{F}_j + \hat{E}_{ij} + \hat{C}_i \tag{12b}$$

The $\hat{E}_{ij}$ are equivalent to those in equation (1).

Equations (12a) and (12b) relate single-station magnitude to network magnitudes. Let us rewrite them as:

$$(\hat{F}_{ij} - \hat{F}_j) = \hat{E}_{ij} \tag{13a}$$

$$(\hat{F}'_{ij} - \hat{F}_j) = \hat{E}_{ij} + \hat{C}_i \tag{13b}$$

We now consider the magnitude differences above as random variables with variances given by:

$$\sigma_i^2(\hat{F}_{ij} - \hat{F}_j) = \sigma_i^2(\hat{E}_{ij})$$

$$\sigma_i^2(\hat{F}_{ij} - \hat{F}_j) = \sigma_i^2(\hat{E}_{ij}) + \sigma_i^2(\hat{C}_j)$$

where the subscript i on σ^2 indicates a summation over stations. From the final iteration of the JMD program, we obtain the variance of all the $\hat{E}_{ij}$'s, and the variance of the $\hat{C}_i$'s is easily obtained from the values of these terms as given in Tables II and V. The computed values of $\sigma_{ij}^2(\hat{E}_{ij})$ are .020 for surface waves and .036 for body waves, and the values of $\sigma_i^2(\hat{C}_i)$ are .046 for surface waves and .150 for body waves. (For the body waves, $\sigma_i^2(\hat{C}_i)$ should be significantly reduced by using line segments or a polynomial to fit the amplitude-distance data.) These values are reflected in Figures 1a and 1b, 2a and 2b, 4a, and 4b which compare scatter before and after station corrections are applied in magnitude estimation.

The $\sigma_{ij}^2(\hat{E}_{ij})$ can also be related to the scatter observed in M_s vs m_b plots for single stations compared to those for networks as in Figures 10a, 10b, and 10c. In each figure the identical event set is used for both single-station and network estimates of magnitude; the events and estimates are listed in Table X. The scatter in the single-station plots is greater, and we can express this quantitatively by forming equation (12a) for both body and surface waves and subtracting to

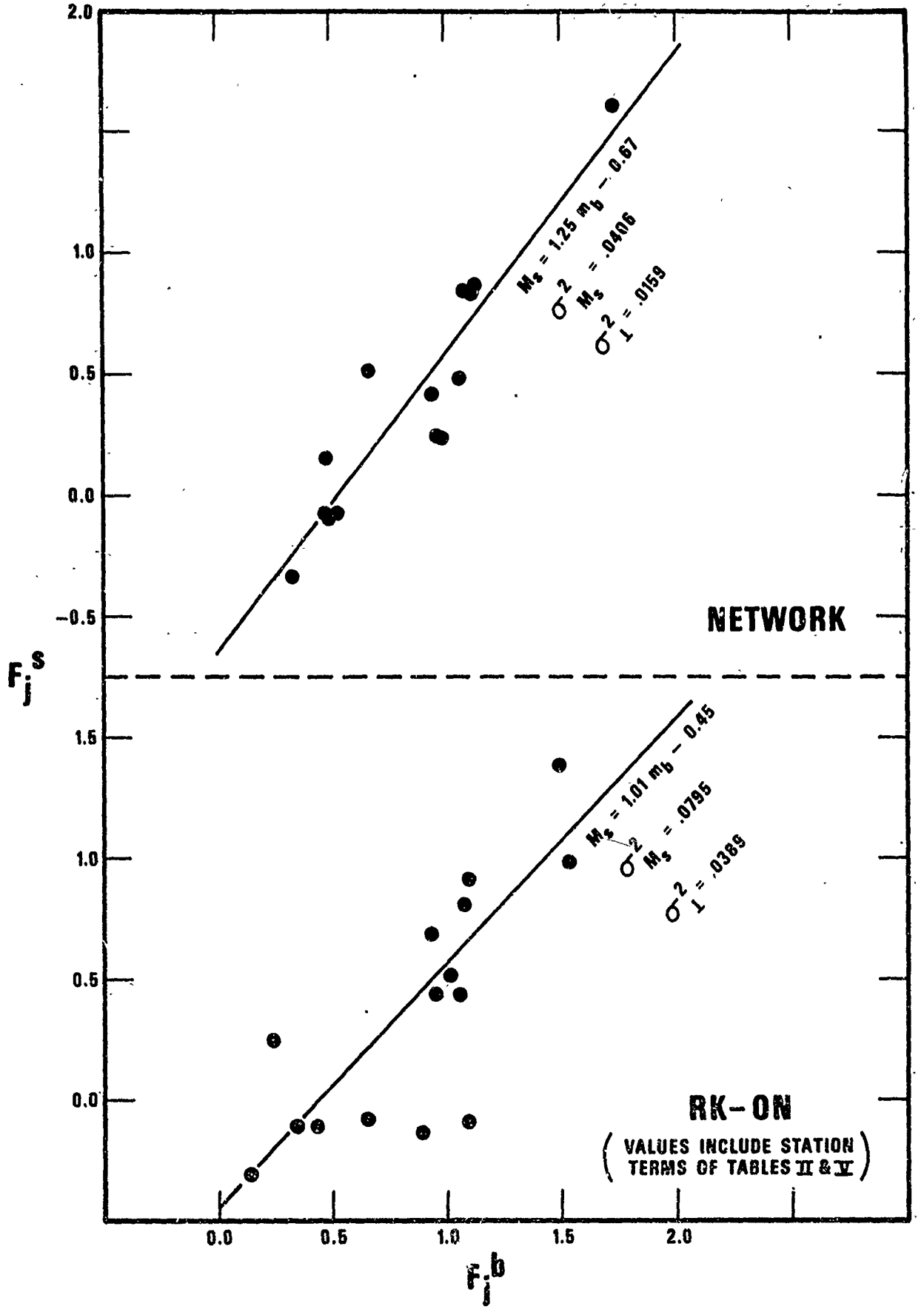

Figure 10a. M_S vs m_b at RK-ON compared to network estimates for same events.

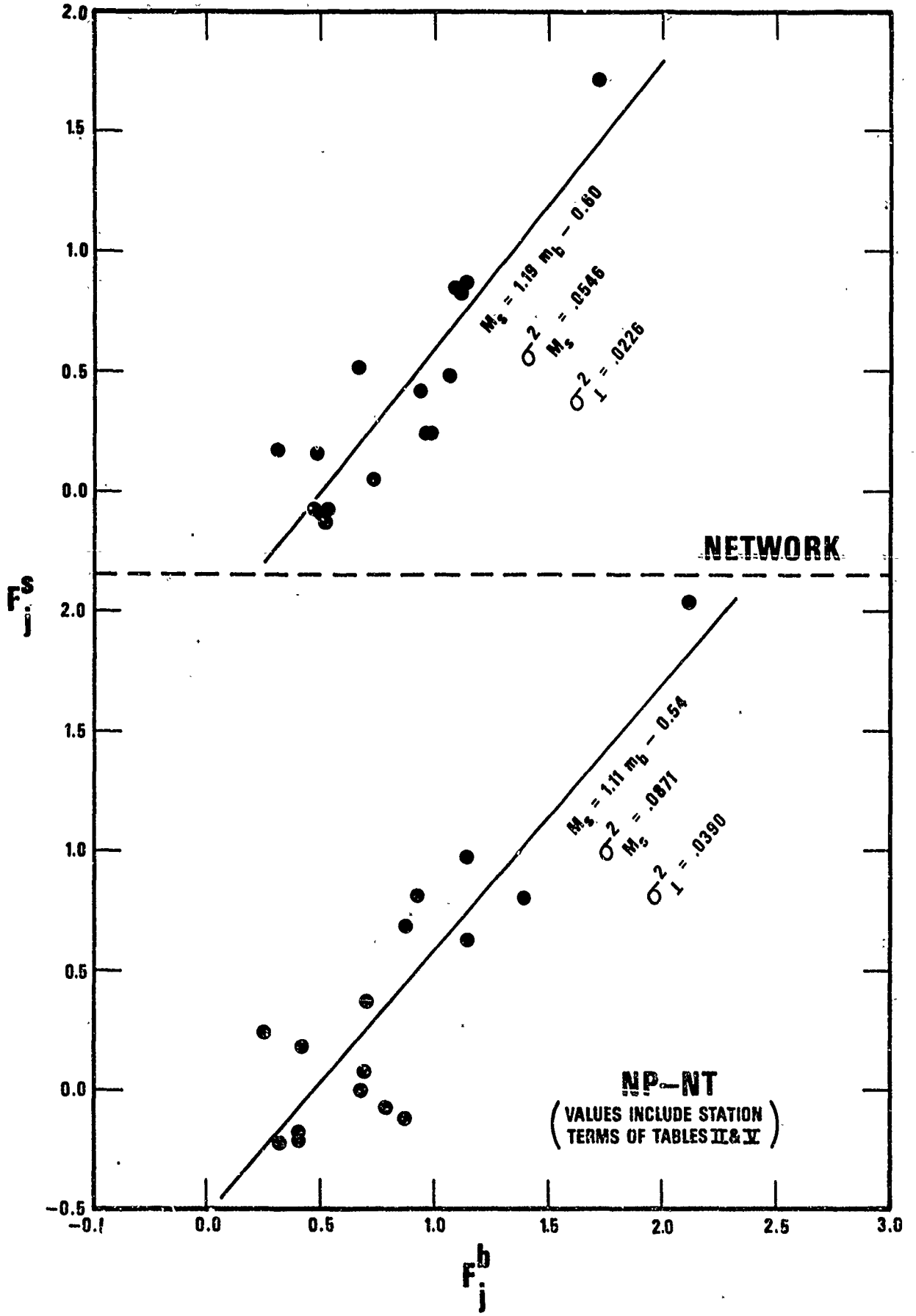

Figure 10b. M_S vs m_b at NP-NT compared to network estimates for same events.

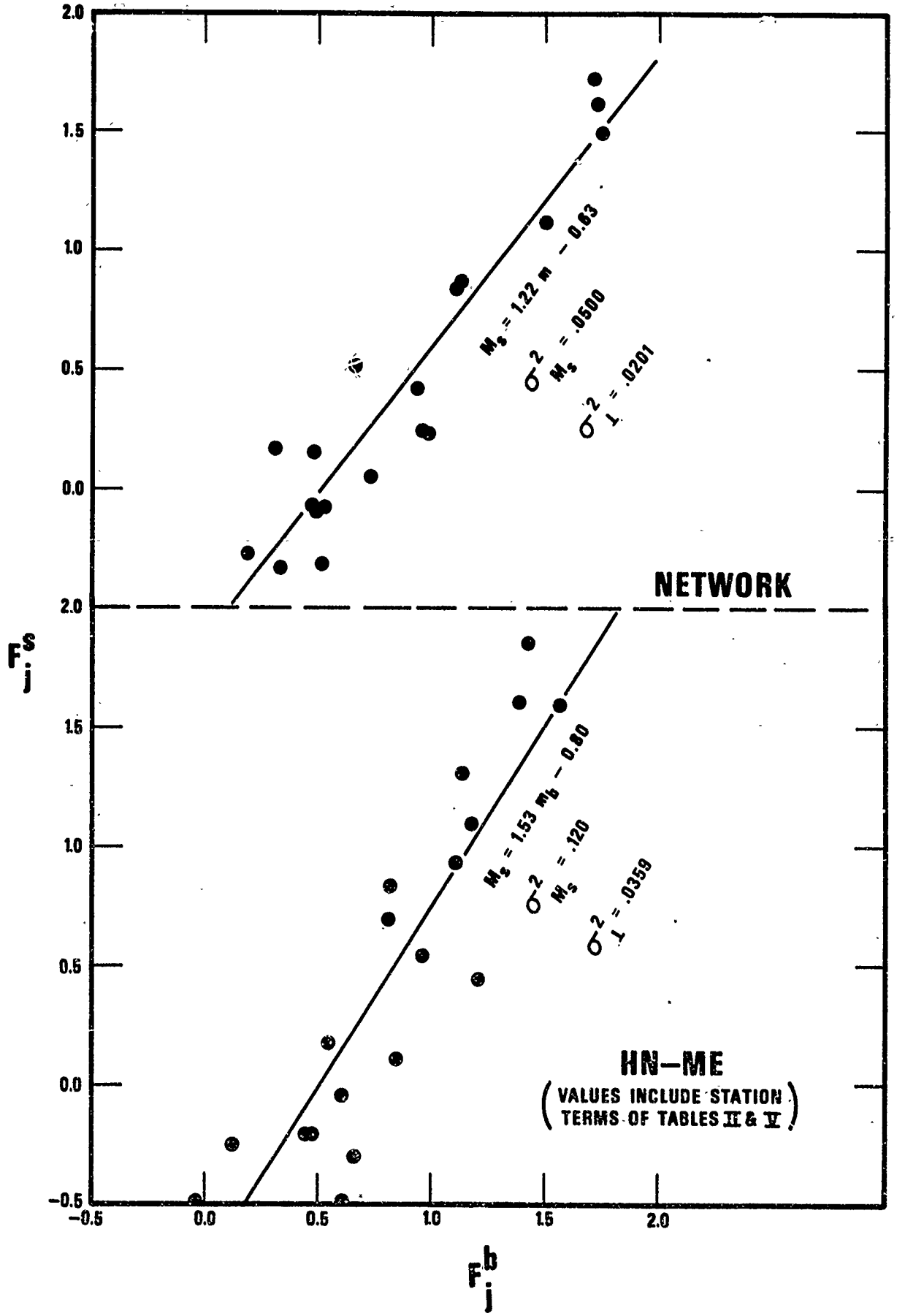

Figure 10c. M_S vs m_b at HN-ME compared to network estimates for same events.

TABLE X

Event Terms C. ulated from Three Single Stations and From Entire Network

	RK-ON		HN-ME		NP-NT		NETWORK*	
	F^s	F^b	F^s	F^b	F^s	F^b	F^s	F^b
BENHAM	1.38+	1.49	1.60	1.39	-	-	1.60	1.73
BILBY	.80	1.07	-	-	.81	.92	.84	1.08
BOURBON	-	-	- .05	.61	.24	.25	.17	.31
BOXCAR	-	-	1.85	1.43	2.04	2.11	1.71	1.72
BRONZE	.24	.24	.10	.85	.18	.42	.15	.48
BUFF	- .11	.34	- .31	.66	- .21	.40	- .08	.52
CHARCOAL	- .31	.14	- .51	.61	-	-	- .34	.33
CHARTREUSE	-	-	.17	.55	- .07	.78	.04	.73
COMMODORE	.91	1.09	.83	.82	.97	1.14	.86	1.13
CORDUROY	.51	1.01	-	-	.62	1.14	.48	1.06
CUP	- .11	.43	- .21	.45	- .18	.40	- .07	.47
DUMONT	.68	.93	.44	1.21	.37	.70	.41	.94
DURYEA	- .14	.89	- .26	.13	- .12	.87	- .10	.49
GREELEY	-	-	1.59	1.57	-	-	1.49	1.75
HALFBEAK	-	-	1.31	1.14	-	-	1.11	1.51
KNICKERBOCKER	.44	.95	.69	.81	.68	.87	.51	.66
MISSISSIPPI	-	-	- .21	.47	-	-	- .32	.52
NASH	-	-	-	-	- .22	.32	- .13	.52
PILEDRIVER	- .08	.65	.54	.96	.07	.69	.23	.98
SCOTCH	.98	1.53	.93	1.11	.80	1.39	.83	1.11
TAN	.43	1.05	1.09	1.18	.00	.67	.24	.97
TURF	-	-	- .49	- .04	-	-	- .28	.19

+All F estimates include C_i terms(s).

*Network estimates are same as given in Tables I and IV.

-Lacks compressional-wave or Rayleigh-wave recording, or both.

obtain:

$$(\hat{F}^s_{ij} - \hat{F}^b_{ij}) = (\hat{F}^s_j - \hat{F}^b_j) + \hat{E}^s_{ij} - \hat{E}^b_{ij}$$

Considering the above magnitude difference as a random variable again, we can express the variance as:

$$\sigma^2_j(\hat{F}^s_{ij} - \hat{F}^b_{ij}) = \sigma^2_j(\hat{F}^s_j - \hat{F}^b_j) + \sigma^2_j(\hat{E}^s_{ij}) + \sigma^2_j(\hat{E}^b_{ij})$$

where the subscript j on σ^2 indicates a summation over events. Using the computed variances of the magnitude differences as given in Figures 10a, 10b, and 10c, we obtain $\sigma^2_j(\hat{E}^s_{ij}) + \sigma^2_j(\hat{E}^b_{ij})$ equal to .039, .033 and .070 for RK-ON, NP-NT and HN-ME respectively. (The computed variances on these figures are for the vertical deviation of the points from the least-squares fitted lines. Using the vertical distance actually gives the variance of $M_s - \alpha\, m_b$ where α is the slope of the fitted line. None of the analysis is seriously affected by values of α which are slightly different from 1.0.) We know from the JMD results that $\sigma^2_{ij}(\hat{E}^s_{ij}) + \sigma^2_{ij}(\hat{E}^b_{ij})$ is .056 for the entire group of data covering more than a hundred stations. Thus RK-ON and NP-NT exhibit less measurement error than at a typical station while HN-ME exhibits more.

From equation (12a) we have shown that scatter for single-station M_s vs m_b plots will exceed that for a network by $\sigma_j^2(\hat{E}_{ij}^s) + \sigma_j^2(\hat{E}_{ij}^b)$ for that particular station when station corrections are applied. When they are not, we must proceed from equation (12b) and let

$$\hat{F}_j = \hat{F}_j' - \frac{1}{L_j} \sum_{i=1}^{L_j} \hat{C}_i \tag{14}$$

where L_j is the number of stations recording the j'th event. Substituting (14) in (12b), forming (12b) for body waves and surface waves again, and subtracting, we obtain:

$$(\hat{F}_{ij}^{s'} - \hat{F}_{ij}^{b'}) = (\hat{F}_j^{s'} - \frac{1}{L_j^s} \sum_{i=1}^{L_j^s} \hat{C}_i^s - \hat{F}_j^{b'} + \frac{1}{L_j^b} \sum_{i=1}^{L_j^b} \hat{C}_i^b)$$

$$+ \hat{E}_{ij}^s - \hat{E}_{ij}^b + \hat{C}_i^s - \hat{C}_i^b$$

We can write the scatter of this magnitude difference as:

$$\sigma_j^2(\hat{F}_{ij}^{s'} - \hat{F}_{ij}^{b'}) = \sigma_j^2(\hat{F}_j^{s'} - \hat{F}_j^{b'} - \frac{1}{L_j^s}\sum_{i=1}^{L_j^s}\hat{C}_i^s + \frac{1}{L_j^b}\sum_{i=1}^{L_j^b}\hat{C}_i^b)$$

$$+ \sigma_j^2(\hat{E}_{ij}^s) + \sigma_j^2(\hat{E}_{ij}^b) \qquad (15)$$

$$+ \sigma_j^2(\hat{C}_i^s) + \sigma_j^2(\hat{C}_i^b)$$

Since $\hat{C}_i$ is constant from event to event, its variance is zero here. By equation (14), $\hat{F}_j'$ is defined as the sum of two random variables, and its scatter must be greater than that of $\hat{F}_j$ so that

$$\sigma_j^2(\hat{F}_j^{s'} - \hat{F}_j^{b'} - \frac{1}{L_j^s}\sum_{i=1}^{L_j^s}\hat{C}_i^s + \frac{1}{L_j^b}\sum_{i=1}^{L_j^b}\hat{C}_i^b) =$$

$$\sigma_j^2(\hat{F}_j^{s'} - \hat{F}_j^{b'}) - \sigma_j^2(\frac{1}{L_j^s}\sum_{i=1}^{L_j^s}\hat{C}_i^s) - \sigma_j^2(\frac{1}{L_j^b}\sum_{i=1}^{L_j^b}\hat{C}_i^b)$$

Applying the above principles to (15), we have

$$\sigma_j^2(\hat{F}_{ij}^{s'} - \hat{F}_{ij}^{b'}) = \sigma_j^2(\hat{F}_j^{s'} - \hat{F}_j^{b'}) + \sigma_j^2(\hat{E}_{ij}^{s})$$

$$+ \sigma_j^2(\hat{E}_{ij}^{b}) - \sigma_j^2\left(\frac{1}{L_j^s}\sum_{i=1}^{L_j^s}\hat{C}_i^s\right) - \sigma_j^2\left(\frac{1}{L_j^b}\sum_{i=1}^{L_j^b}\hat{C}_i^b\right)$$

Using the fact that the variance of the mean of L_j realizations of a random variable is equal to $1/L_j$ times the variance of the variable itself, this reduces to:

$$\sigma_j^2(\hat{F}_{ij}^{s'} - \hat{F}_{ij}^{b'}) = \sigma_j^2(\hat{F}_j^{s'} - \hat{F}_j^{b'}) + \sigma_j^2(\hat{E}_{ij}^{s})$$

$$+ \sigma_j^2(\hat{E}_{ij}^{b}) - \frac{1}{L_j^s}\sigma_i^2(\hat{C}_i^s) - \frac{1}{L_j^b}\sigma_i^2(\hat{C}_i^b) \qquad (16)$$

This relation shows that, when station corrections are not applied and the network has a large number of stations, the scatter of a single-station M_s vs m_b plot will exceed that of a network by the combined variance of the measurement error as in the case when station

corrections are applied. However, if L_j^s or L_j^b is small and station corrections are relatively large compared to measurement errors the single-station plot may actually have less scatter than the network plot.

We desire to add still another noise term to our analysis by letting $\hat{F}_j$ be a linear function of the logarithm of yield plus a random variable $\hat{S}_j$ which is the aberration from the expected magnitude for a given yield due to detonation depth, source medium, and possibly tectonic strain-release influences. For a real event, there may be some variation of the $\hat{S}_j$ among stations due to a dependency of this factor on azimuth and take-off angle of the ray path at the source, but we will disregard such variation in this discussion. In fact, if such variation in $\hat{S}_j$ is consistent among events, it will be absorbed by the $\hat{C}_i$ terms. The $\hat{S}_j$'s are estimatible only if the yields are known; however, we can estimate the variance of the $\hat{S}_j$'s without yield information. The linear relation between magnitude and yield has a substantial theoretical and empirical basis up to approximately 100 kt or $m_b \approx 6$ (von Seggern and Lambert, 1970; Liebermann and Pomeroy, 1969; Evernden, 1969; Evernden and Filson, 1971; Ericsson, 1971). From these studies, the coefficient on the logarithm of yield ranges from approximately 0.8 to 1.2. Without any significant effect on our results we can assume it is 1.0 for both body and surface waves. We make these definitions then:

$$\hat{F}_j = \log Y_j + K + \hat{S}_j + \frac{1}{L_j} \sum_{i=1}^{L_j} \hat{E}_{ij} \qquad (17a)$$

$$\hat{F}'_j = \log Y_j + K + \hat{S}_j + \frac{1}{L_j}\sum_{i=1}^{L_j}\hat{E}_{ij} + \frac{1}{L_j}\sum_{i=1}^{L_j}\hat{C}_i \qquad (1$$

These definitions include the mean of the measurement error terms since the JMD estimate of $\hat{F}_j$ will necessarily be biased by this value, and we do not want to include it in the source term $\hat{S}_j$. If we form (17a) and (17b) for both body and surface waves and subtract, we obtain:

$$\hat{F}^s_j - \hat{F}^b_j + K^s - K^b = \hat{S}^s_j - \hat{S}^b_j + \frac{1}{L^s_j}\sum_{i=1}^{L^s_j}\hat{E}^s_{ij} - \frac{1}{L^b_j}\sum_{i=1}^{L^b_j}E^b_{ij} \qquad (18a)$$

$$\hat{F}^{s\prime}_j - \hat{F}^{b\prime}_j + K^s - K^b = \hat{S}^s_j - \hat{S}^b_j + \frac{1}{L^s_j}\sum_{i=1}^{L^s_j}\hat{E}^s_{ij} - \frac{1}{L^b_j}\sum_{i=1}^{L^b_j}\hat{E}^b_{ij} + \frac{1}{L^s_j}\sum_{i=1}^{L^s_j}\hat{C}^s_i - \frac{1}{L^b_j}\sum_{i=1}^{L^b_j}\hat{C}^b_i \qquad (18b)$$

The scatter of these magnitude differences is:

$$\sigma_j^2(\hat{F}_j^s - \hat{F}_j^b) = \sigma_j^2(\hat{S}_j^s) + \sigma_j^2(\hat{S}_j^b) + \frac{1}{L_j^s}\,\sigma_i^2(\hat{E}_{ij}^s) + \frac{1}{L_j^b}\,\sigma_i^2(\hat{E}_{ij}^b) \tag{19a}$$

$$\sigma_j^2(\hat{F}_j^{s'} - \hat{F}_j^{b'}) = \sigma_j^2(\hat{S}_j^s) + \sigma_j^2(\hat{S}_j^b) + \frac{1}{L_j^s}\,\sigma_i^2(\hat{E}_{ij}^s) + \frac{1}{L_j^b}\,\sigma_j^2(E_{ij}^b) + \frac{1}{L_j^s}\,\sigma_i^2(\hat{C}_i^s) + \frac{1}{L_j^b}\,\sigma_i^2(\hat{C}_i^b) \tag{19b}$$

where again, as in arriving at (16), we used the fact that the variance of the mean is $1/L_j$ times the variance of the variable itself.

We can now estimate the variance of the source terms by applying equation (19a) to the JMD results shown in Figure 7. There the variance of the points about the

fitted line, measured vertically, is approximately .037. Variances on other M_s vs m_b plots for these same events in Figures 5, 6, 8 and 9 are within 20 percent of this value. On the average, $L_j^s = 17$ and $L_i^b = 20$ for the 36 events of Figure 7; and using $\sigma_i^2(\hat{E}_{ij}^s) = .020$ and $\sigma_i^2(\hat{E}_{ij}^b) = .036$ in equation (19a), we estimate the combined source variance to be .034. Since we have no means of separating the two, we simply assume $\sigma_j^2(\hat{S}_j^s) = \sigma_j^2(\hat{S}_j^b) = .017$. With yield information Ericsson was able to make the separation and obtained $\sigma_j^2(\hat{S}_j^s) = .012$ and $\sigma_j^2(\hat{S}_j^b) = .017$ for his data. It is noteworthy that the six explosions which Ericsson used were all detonated within a small test area on Pahute Mesa in either a rhyolite or tuff medium and that the 36 explosions considered in this report were detonated over a much greater area and in a variety of media. On that basis, we expect $\sigma_j^2(\hat{S}_j)$ to be much larger for our group, but it is in fact only slightly so.

We now can explain the failure of station corrections to improve the network M_s vs m_b scatter as shown by Figures 6 and 7. Equation (19b) applies to Figure 6, while equation (19a) applies to Figure 7. Using $\sigma_i^2(\hat{C}_i^s) = .046$ and $\sigma_i^2(\hat{C}_i^b) = .150$ as previously determined, we see that since these are divided by the number of stations, their combined weight in equation (19b) is about one-third to one-fourth the combined weight of $\sigma_j^2(\hat{S}_j^s)$ and $\sigma_j^2(\hat{S}_j^b)$, with the measurement variances also relatively small. It is evident, though, that their weight will increase as the number of stations decreases, so that station corrections are imperative when small changing networks or random isolated stations record events.

CONCLUSIONS

The JMD method of magnitude estimation is a simple and straightforward procedure which performs as well as routine magnitude estimation. This is shown by the fact that M_s vs m_b plots show about the same scatter when JMD results for 36 NTS explosions were compared against routine ones. Because of its manner of incorporating distance effects into station corrections, the method can only be applied uniformly to a limited source region, perhaps only a hundred kilometers wide.

Both Rayleigh-wave and compressional-wave amplitudes from NTS explosions were shown to be log-normally distributed over a large station network. This fact considerably simplifies the statistical model for magnitudes and justifies the traditional procedure of averaging station magnitudes to obtain an event magnitude estimate.

In our analysis of variance for M_s and m_b, we found:

$$\text{var(surface-wave measurement noise)} = .020 = \text{var}(\hat{E}_{ij}{}^{s})$$

$$\text{var(body-wave measurement noise)} = .036 = \text{var}(\hat{E}_{ij}{}^{b})$$

$$\text{var(surface-wave path station noise)} = .046 = \text{var}(\hat{C}_{i}{}^{s})$$

$$\text{var(body-wave path station noise)} = .150 = \text{var}(\hat{C}_{i}{}^{b})$$

$$\text{var(surface-wave source noise)} = .017 = \text{var}(\hat{S}_{j}{}^{s})$$

$$\text{var(body-wave source noise)} = .017 = \text{var}(\hat{S}_{j}{}^{b})$$

One can estimate these variances without the knowledge of the explosive yields provided there is a sufficient number of events and stations to apply statistical procedures reliably. We emphasize that these results apply only to the data base used here -- LRSM stations and NTS explosions -- and may change significantly with other data bases.

Of the three types of noise, the station-path term $\hat{C}_i$ is predominant. Its biasing of magnitude can be eliminated entirely by repeated use of a single station or of an identical group of stations to estimate event magnitudes; in this case all magnitudes will be biased by an equal amount and thus not contribute to scatter in M_s vs m_b. Its biasing effect can also be suppressed by use of well-determined station corrections. If the $\hat{E}_{ij}$ term can be kept small by accurate recording system calibration and careful systematic measurements, even a single station could give M_s vs m_b plots with a small scatter. This can be observed for Berkeley recordings (McEvilly, 1971) and Lamont recordings (Savino, 1971). When compelled to use varying stations or networks for magnitude estimation, as many stations as possible should be used because the effect of the $\hat{C}_i$ term is reduced by increasing the number of stations. This holds for the $\hat{E}_{ij}$ term also. If a large number of stations are used, say ten or more, then the application of station corrections clearly becomes superfluous in reducing M_s vs m_b scatter.

The source-term variance $\hat{S}_j$ cannot be suppressed and is the primary remaining cause of M_s vs m_b scatter. This

alone gives a standard deviation of 0.13 units normal to the M_s vs m_b straight-line fit for the NTS data (assuming a slope of unity). We feel that this is less than the scatter that could result if a conscious continuing attempt were made to select the detonation media and depth in such a way as to vary the source coupling in short and long periods. An examination of source medium and depth effects on M_s and m_b coupling seems essential if we are to define the expected limits of possible scatter in explosion M_s vs m_b plots for a selected test region.

REFERENCES

Basham, P.W., 1971, A new magnitude formula for short period continental Rayleigh waves, Geophys. J.R. Astr. Soc., v. 23, p. 255-260.

Båth, Markus, 1966, Earthquake energy and magnitude, in Physics and Chemistry of the Earth, v. 7, Pergamon Press, New York.

Båth, Markus, 1969, Handbook on earthquake magnitude determinations (second edition), VESIAC Special Report No. 7885-36-X, University of Michigan, Institute of Science and Technology.

Douglas, A., 1967, Joint epicenter determination, Nature, v. 215, p. 47-48.

Ericsson, Ulf, 1971, A linear model for the yield dependence of magnitudes measured by a seismographic network, Geophys. J.R. Astr. Soc., in press.

Evernden, J., 1967, Magnitude determination at regional and near-regional distances in the United States, Bull. Seismol. Soc. Amer., v. 57, p. 591-637.

Evernden, Jack F. and Filson, John, 1971, Regional dependence of surface-wave versus body-wave magnitudes, J. Geophys. Res., v. 76, p. 3303-3308.

Freedman, Helen, 1967, Estimating earthquake magnitude, Bull. Seismol. Soc. Amer., v. 57, p. 747-760.

Gutenberg, B., 1945a, Amplitudes of surface waves and magnitude of shallow earthquakes, Bull. Seismol. Soc. Amer., v. 35, p. 3-12.

REFERENCES (Cont'd.)

Gutenberg, B., 1945b, Amplitudes of P, PP, and S and magnitude of shallow earthquakes, Bull. Seismol. Soc. Amer., v. 35, p. 57-69.

Gutenberg, B. and Richter, C.F., 1956, Magnitude and energy of earthquakes, Annali Geofisica, v. 9, p. 1-15.

Klappenberger, F.A., 1967, Distribution of short-period P-phase amplitudes over LASA, Seismic Data Laboratory Report No. 187, Teledyne Geotech, Alexandria, Virginia.

Lambert, D.G., 1971, Relationship of body and surface wave magnitudes for small earthquakes and explosions, Seismic Data Laboratory Report No. 245, Teledyne Geotech, Alexandria, Virginia.

Liebermann, Robert C. and Pomeroy, Paul W., 1969, Relative excitation of surface waves by earthquakes and underground explosions, J. Geophys. Res., v. 74, p. 1575-1590.

Lilliefors, Hubert W., 1967, On the Kolmogorov-Smirnov test for normality with mean and variance unknown, J. Amer. Statist. Assc., v. 62, p. 399-402.

McEvilly, T. V., 1971, Explosions/afterevents/earthquakes -- characteristics at short (500-600 km) and very short distances, ARPA Symposium on Seismic Discrimination, v. II, Woods Hole, Massachusetts.